EUROPEAN ORGANIZATION FOR NUCLEAR RESEARCH (CERN)

CERN-EP-2017-102
2017/08/29

CMS-B2G-15-006

Search for top quark partners with charge 5/3 in proton-proton collisions at $\sqrt{s} = 13\,\text{TeV}$

The CMS Collaboration*

Abstract

A search for the production of heavy partners of the top quark with charge 5/3 ($X_{5/3}$) decaying into a top quark and a W boson is performed with a data sample corresponding to an integrated luminosity of 2.3 fb^{-1}, collected in proton-proton collisions at a center-of-mass energy of 13 TeV with the CMS detector at the CERN LHC. Final states with either a pair of same-sign leptons or a single lepton, along with jets, are considered. No significant excess is observed in the data above the expected standard model background contribution and an $X_{5/3}$ quark with right-handed (left-handed) couplings is excluded at 95% confidence level for masses below 1020 (990) GeV. These are the first limits based on a combination of the same-sign dilepton and the single-lepton final states, as well as the most stringent limits on the $X_{5/3}$ mass to date.

Published in the Journal of High Energy Physics as doi:10.1007/JHEP08(2017)073.

*See Appendix A for the list of collaboration members

1 Introduction

Various extensions of the standard model (SM) predict new heavy particles for addressing the hierarchy problem caused by the quadratic divergences in the quantum-loop corrections to the Higgs boson (H) mass. The largest corrections, owing to the top quark loop, are canceled in many of these models, for example composite Higgs models [1–4], by the presence of heavy partners of the top quark. This paper describes a search for such spin 1/2 top quark partners, using data collected by the CMS experiment at $\sqrt{s} = 13\,\text{TeV}$ in 2015. We focus on a top quark partner with exotic charge +5/3 (in units of the absolute charge of the electron). Such exotically charged fermions need not necessarily contribute to the coupling of the Higgs boson to gluons [5], and thus the measurements of the Higgs production rates at the LHC set no constraint on the $X_{5/3}$ particle. While our previous searches and other literature referred to this particle as $T_{5/3}$, in this paper we follow the nomenclature of Ref. [1] and refer to it as $X_{5/3}$.

The color charge of the $X_{5/3}$ quark allows it to be produced via quantum chromodynamics (QCD) interactions in proton-proton collisions with leading-order cross sections that depend on new physics only via the $X_{5/3}$ mass. We assume that the $X_{5/3}$ quark decays via $X_{5/3} \to tW^+$ followed by $t \to W^+b$ (charge conjugate modes are implied throughout), which is the dominant decay mode in most models. Because mixing of the $X_{5/3}$ quark with the top quark only occurs through the weak interaction, production via QCD processes always results in the production of $X_{5/3}$ pairs (particle and antiparticle), as shown in Fig. 1. The $X_{5/3}$ quark can also be produced singly in association with a top quark through electroweak processes; however, this production mode is not considered here.

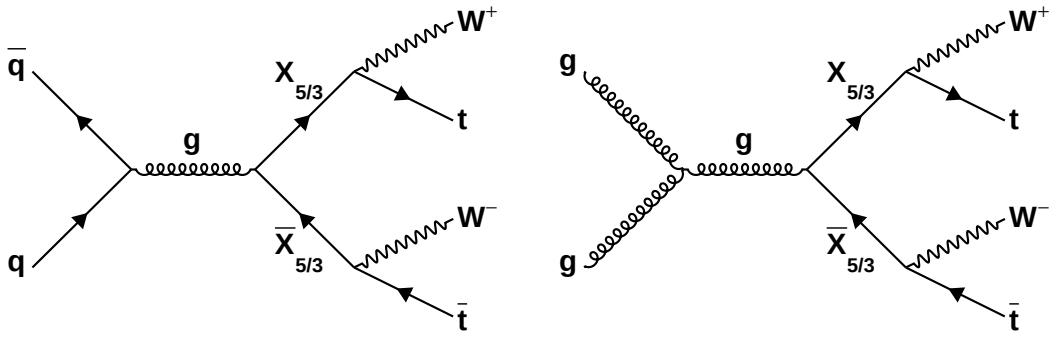

Figure 1: Leading order Feynman diagrams for the production and decay of pairs of $X_{5/3}$ particles via QCD processes.

In this paper, the search for the $X_{5/3}$ particle is focused on two final states. In the "same-sign dilepton channel" the two (same-charge) W bosons arising from one of the $X_{5/3}$ particles decay into leptons of the same charge while the other two W bosons decay inclusively. In the "single-lepton channel", one of the W bosons decays leptonically into a lepton and a neutrino, while the other three W bosons decay hadronically (including $W \to \tau \to$ hadrons). Throughout the paper, when referring to a lepton (ℓ), we mean either an electron or muon. In both channels, leptonic decays from taus are included in the signal region although the lepton identification criteria are optimized for direct decays to either electrons or muons.

A previous search in the same-sign dilepton channel conducted by CMS, using $19.5\,\text{fb}^{-1}$ of data collected at $\sqrt{s} = 8\,\text{TeV}$, set a lower limit on the $X_{5/3}$ mass of 800 GeV [6] at 95% confidence level (CL). Searches have also been performed by the ATLAS experiment using $20.3\,\text{fb}^{-1}$ of data collected at $\sqrt{s} = 8\,\text{TeV}$ in the same-sign dilepton [7] and single-lepton [8] final states

separately, setting lower limits of 740 and 840 GeV, respectively.

2 The CMS detector

The central feature of the CMS apparatus is a superconducting solenoid of 6 m internal diameter, providing a magnetic field of 3.8 T. Within the solenoid volume are a silicon pixel and strip tracker, a lead tungstate crystal electromagnetic calorimeter (ECAL), and a brass and scintillator hadron calorimeter (HCAL), each composed of a barrel and two endcap sections. Forward calorimeters extend the pseudorapidity (η) coverage provided by the barrel and endcap detectors. Muons are measured in gas-ionization detectors embedded in the steel flux-return yoke outside the solenoid. The first level of the CMS trigger system, composed of custom hardware processors, selects the most interesting events in a fixed time interval of less than 4 μs, using information from the calorimeters and muon detectors. The high-level trigger processor farm further decreases the event rate to a few hundred Hz, before data storage. A more detailed description of the CMS detector, together with a definition of the coordinate system used and the relevant kinematic variables, can be found in Ref. [9].

3 Simulation

The $X_{5/3}$ signal processes are generated using a combination of MADGRAPH5_aMC@NLO 2.2.2 [10] and MADSPIN [11] for two coupling scenarios, corresponding to purely left- or right-handed $X_{5/3}$ coupling to W bosons, denoted by LH and RH, respectively. The MADGRAPH generator is used both to produce $X_{5/3}$ events and decay each $X_{5/3}$ to a top quark and a W boson, while the decays of the top quarks and W bosons are simulated with MADSPIN. The signal events are simulated at leading order (LO) for various mass values between 700 and 1600 GeV in 100 GeV steps, separately for each coupling scenario. The $X_{5/3}$ cross sections are then normalized to the next-to-next-to-leading order using Top++2.0 [12–17].

The Monte Carlo (MC) background processes are generated with a variety of event generators. The MADGRAPH5_aMC@NLO event generator is used to simulate Z+jets, W+jets, single top in the s- and t-channels, $\mathrm{t\bar{t}Z}$, $\mathrm{t\bar{t}W}$, $\mathrm{t\bar{t}H}$, and $\mathrm{t\bar{t}t\bar{t}}$ processes, as well as events with a combination of three W or Z bosons and QCD multijet events. The W+jets and multijet events are generated at LO using the MLM matching scheme [18], while the others are simulated to next-to-leading order (NLO) using the MLM matching scheme, except for Z+jets and $\mathrm{t\bar{t}W}$ where the FxFx matching scheme [19] is used. The POWHEG 2.0 [20–23] event generator is used to simulate $\mathrm{t\bar{t}}$ and single top quark events in the tW channel at NLO accuracy. The diboson events involving W or Z are generated at LO using either MADGRAPH5_aMC@NLO or PYTHIA 8.212 [24, 25]. Parton showering, hadronization, and the underlying event are simulated with PYTHIA, using NNPDF 3.0 [26] parton distribution functions (PDF) with the CUETP8M1 underlying event tune [27].

All MC events are processed with GEANT4 [28, 29] for a full simulation of the CMS detector. Further, for all simulated samples, additional proton-proton interactions (pileup) are modeled by superimposing generated minimum bias interactions onto both the bunch crossing of the simulated events and also in adjacent bunch crossings. A reweighting procedure is used to match the simulated distributions to the number of pileup interactions observed in data.

4 Object reconstruction

The analyses described in this paper rely on the reconstruction of four types of objects: electrons, muons, jets, and missing transverse energy ($E_{\mathrm{T}}^{\mathrm{miss}}$). Events are reconstructed using the particle-flow (PF) approach [30], which consists of reconstructing and identifying each single particle with an optimized combination of all subdetector information. The details of the object selection are provided below.

Candidate events are required to have at least one reconstructed vertex. For events in which there are multiple reconstructed vertices, the one with the the largest sum of squared transverse momenta of associated tracks is chosen as the primary vertex. For the dilepton analysis, at least two leptons are required to be within the tracker acceptance ($|\eta| < 2.4$) and to have passed triggers based on dielectron, dimuon or electron-muon requirements. All double lepton triggers used have an $|\eta| < 2.4$ requirement and p_{T} requirements ranging from 17 to 27 GeV on the leading lepton and from 8 to 12 GeV on the sub-leading lepton. The single-lepton analysis requires events to have passed a single-electron trigger ($|\eta| < 2.1$, $p_{\mathrm{T}} > 27$ GeV) or a single-muon trigger ($|\eta| < 2.4$, $p_{\mathrm{T}} > 20$ GeV).

Electron candidates are reconstructed from a collection of electromagnetic clusters and matched to tracks in the tracker [31]. They are then required to satisfy identification and isolation criteria. The identification criteria make use of shower shape variables, track quality requirements, the distance from the track to the primary vertex, and variables measuring compatibility between the track and matched electromagnetic clusters to select good electron candidates. Requirements are also imposed to reject electrons produced in photon conversions in the detector material. The isolation variable (I_{mini}) is defined as the sum of energy around the electron in a cone of varying size, divided by the transverse momentum (p_{T}) of the electron. The radius used for the isolation cone (R) is defined as:

$$R = \frac{10\,\mathrm{GeV}}{\min[\max(p_{\mathrm{T}}, 50\,\mathrm{GeV}), 200\,\mathrm{GeV}]}\,.$$

We define a "tight" ("loose") electron to have $I_{\mathrm{mini}} < 0.1\,(0.4)$.

For the same-sign dilepton analysis, charge misidentification is significantly reduced by requiring that different charge measurements for an electron agree (a $\sim$50% reduction is possible for requiring all measurements agree for low p_{T} electrons). Two of the measurements are based on two different tracking algorithms: the standard CMS track reconstruction algorithm [32] and the Gaussian-sum filter algorithm [33], optimized to take into account the possible emission of bremsstrahlung photons in the silicon tracker. The third measurement is based on the relative position of the calorimeter cluster and the projected track from the pixel detector seed (the pixel hits used to reconstruct an electron's track). We find good agreement between the three measurements for electrons with $p_{\mathrm{T}} < 100$ GeV. However, for higher-momentum electrons, requiring that the third measurement agree with the two track-based determinations leads to a 5–10% loss in signal efficiency. Further, the third measurement is also often incorrect for high p_{T} electrons. We therefore define a "relaxed" charge consistency requirement where for electrons with p_{T} below 100 GeV all three charge measurements are required to agree, while above 100 GeV only the first two measurements are required to agree and the third charge measurement is ignored.

Muons are reconstructed using a global track fit of hits in the muon detectors and hits in the silicon tracker. The track associated with a muon candidate is required to have at least six hits in the silicon tracker, at least one pixel detector hit, and a good quality global fit, including at least one hit in the muon detector. The isolation variable for muons is calculated in the

same way as it is for electrons, as described above. We define a category of "tight" muons that satisfy $I_{\text{mini}} < 0.2$. A second category of "loose" muons requires $I_{\text{mini}} < 0.4$ with somewhat relaxed identification requirements. Additional requirements are imposed on the minimum longitudinal distance of the tracker track with respect to the primary vertex ($d_z < 5\,\text{mm}$) and the minimum radial distance from the track to the primary vertex ($d_{\text{xy}} < 2\,\text{mm}$).

An event-by-event correction using the effective area method [34] is applied to the computation of the electron and muon isolation in order to account for the effect of pileup. Scale factors to correct for imperfect detector simulation are obtained using the "tag-and-probe" method [35] for lepton identification and isolation, as a function of lepton p_{T} and η. These scale factors are normally within a few percent of unity and those falling outside that range tend to be consistent with unity.

Jets are clustered from the reconstructed PF candidates using the anti-k_t algorithm [34, 36–38] with a distance parameter of 0.4 (AK4) and are required to satisfy $p_{\text{T}} > 30\,\text{GeV}$ and $|\eta| < 2.4$. Additional selection criteria are applied to remove spurious features originating from isolated noise patterns in certain HCAL regions and from anomalous signals caused by particles depositing energy in the silicon avalanche photodiodes used in the ECAL barrel region. Jets that overlap with leptons have the leptons removed by matching lepton PF candidates to jet constituents and subtracting the energy and momentum of the matched candidates from the jet four-vector. Jet energy corrections are applied for residual nonuniformity, nonlinearity of the detector response, and the level of pileup in the event [39].

The missing transverse momentum ($\vec{p}_{\text{T}}^{\text{miss}}$) is reconstructed as the negative of the vector p_{T} sum of all reconstructed PF candidates in an event and its magnitude is denoted as $E_{\text{T}}^{\text{miss}}$. Energy scale corrections applied to jets are also propagated to $E_{\text{T}}^{\text{miss}}$.

5 Same-sign dilepton final state

The $X_{5/3}$ search in the dilepton channel takes advantage of the same-sign leptons in the final state as well as the significant amount of jet activity due to the presence of the two bottom quarks and the possibility of hadronic decays for one of the top quark partners.

The background contributions associated with this channel fall into three main categories:

- Same-sign prompt (SSP) leptons: SM processes leading to prompt, same-sign dilepton signatures, where a prompt lepton is defined as one originating from the prompt decay of either a W or Z boson. Their contribution is obtained from simulation.
- Opposite-sign prompt leptons: prompt leptons can be misreconstructed with the wrong charge leading to a same-sign dilepton final state. This contribution is estimated using a data-driven method.
- Same-sign events arising from the presence of one or more non-prompt leptons: this is the primary instrumental background arising from jets misidentified as leptons, non-prompt leptons from heavy flavor decays, fake leptons from conversions, etc. This contribution is also estimated using a data-driven method.

After requiring two tight, same-sign leptons with $p_{\text{T}} > 30\,\text{GeV}$ we impose the following requirements:

- Quarkonia veto: require invariant dilepton mass $M_{\ell\ell} > 20\,\text{GeV}$.
- Associated Z boson veto: ignore any event where $M_{\ell\ell'}$ is within 15 GeV of the mass of the Z boson, where ℓ is either lepton in the same-sign pair, and ℓ' is any lepton not

in the same-sign pair, but of the same flavor as the first, and with $p_T > 30\,\text{GeV}$.

- Primary Z boson veto: events are rejected if $76.1 < M_{\ell\ell} < 106.1\,\text{GeV}$ for the dielectron channel only. If the muon charge is mismeasured, its momentum will also be mismeasured, so a selected muon pair from a Z boson is unlikely to fall within this invariant mass range.
- Leading lepton $p_T > 40\,\text{GeV}$.
- Number of constituents $\geq$5.
- $H_T^{\text{lep}} > 900\,\text{GeV}$.

The "number of constituents" is defined as the number of AK4 jets in the event passing our jet selection together with the number of other (i.e. not in the same-sign pair) tight leptons with $p_T > 30\,\text{GeV}$. The H_T^{lep} used in this analysis is the scalar sum of the p_T of all selected jets and tight leptons in the event. With these requirements we find typical signal efficiencies of roughly 40 to 50% and background rejection of greater than 99%.

5.1 Background modeling

5.1.1 Same-sign prompt lepton background

The same-sign prompt lepton background consists of contributions from diboson production (WZ and ZZ) and rarer processes, such as $t\bar{t}W$, $t\bar{t}Z$, $t\bar{t}H$, WWZ, ZZZ, WZZ, and WW+jets. Many of these processes have not been observed at the LHC or are not yet well measured. We estimate the contribution from SM events with two prompt same-sign leptons using simulation (see Table 1).

5.1.2 Opposite-sign prompt lepton background

Processes with two oppositely-charged prompt leptons can contribute to the background if the charge of one of the leptons is incorrectly measured (this background is referred to throughout as "ChargeMisID"). For muons in the p_T range considered in this analysis, the charge misidentification probability is found to be negligible [40]. For electrons, the magnitude of this contribution can be derived from data by using a sample dominated by Z+jets events. The measurement is performed by first selecting pairs of electrons, with each electron of the pair being in the same $|\eta|$ region and having $p_T < 100\,\text{GeV}$. Each pair is then required to have an invariant mass within 10 GeV of the Z boson mass. Since the momentum and energy measurements of the electrons are driven by the ECAL information, the pair's invariant mass is insensitive to potential track mismeasurement. Counting the number of pairs with same-sign charges then provides the charge misidentification probability as a function of $|\eta|$ for electrons with $p_T < 100\,\text{GeV}$. Next, pairs are formed using one electron with p_T less than 100 GeV and one above 100 GeV. Again the number of same-sign pairs is counted to determine the charge misidentification probability; making use of the previously measured probability for electrons with $p_T < 100\,\text{GeV}$ then gives a measurement of the charge misidentification probability, as a function of $|\eta|$, for electrons with $p_T > 100\,\text{GeV}$. This separate measurement captures the effect of the charge consistency requirement being relaxed at high p_T (as described in Section 4) on the charge misidentification rate. We find values for this probability ranging from 10^{-4} for low p_T electrons in the central part of the detector to a few percent for high p_T electrons in the forward region of the detector.

The number of expected same-sign events due to charge misidentification is estimated by considering the total number of events passing the full selection but having oppositely charged leptons. These events are weighted by the charge misidentification probability parametrized

as a function of $|\eta|$. The resulting expected contribution of same-sign events due to charge misidentification is given in Table 1. A systematic uncertainty of 30% for this background is assigned based on the variation of the charge misidentification probability observed between simulated Drell–Yan (DY) and $\mathrm{t\bar{t}}$ MC events and also taking into account any potential p_{T} dependence for the statistically limited high-p_{T} region.

5.1.3 Same-sign non-prompt background

In this category we consider non-prompt leptons that come from heavy-flavor decays, jets misidentified as leptons, decays in flight, or photon conversions. These contributions are estimated using the "Tight-Loose" method described in Ref. [41] and used in our earlier publication [6]. This method relies on two definitions of leptons: "tight" and "loose", which are described in Section 4.

Any lepton passing either the tight or the loose selection can originate either from a prompt decay or from a non-prompt source, such as a heavy-flavor hadron, a misidentified hadron, or a photon converting to electrons. We refer to the former as "prompt" leptons and to the latter as "fake" leptons. The background is estimated by using events with one or more loose leptons weighted by the ratios of the numbers of tight leptons to the numbers of loose leptons expected for prompt and non-prompt leptons. The ratio for prompt leptons is determined from observed DY events where the invariant mass of the leptons is within 10 GeV of the Z boson mass. We find a prompt rate of 0.873 ± 0.001 for electrons (p_{e}) and of 0.963 ± 0.001 for muons (p_{μ}), where each reported error is the measurement's statistical error. The "fake rate", f_{ℓ}, is defined as the probability that a fake lepton that passes the loose requirements will also pass the tight requirements. It is determined using a data sample enriched in non-prompt leptons. To reduce the contribution of leptons from W and Z boson decays, exactly one loose lepton is required. We also require at least one jet with $p_{\mathrm{T}} > 30\,\mathrm{GeV}$ and $\Delta R > 1.0$ relative to the lepton, $E_{\mathrm{T}}^{\mathrm{miss}} < 25\,\mathrm{GeV}$, and $M_T < 25\,\mathrm{GeV}$, where ΔR is defined as $\sqrt{(\Delta\phi)^2 + (\Delta\eta)^2}$, ϕ is the azimuthal angle measured in radians, and M_T is the transverse mass of the lepton and $\vec{p}_{\mathrm{T}}^{\,\mathrm{miss}}$. We also reject events if the invariant mass of the lepton and any jet is between 81 and 101 GeV. Fake rates of 0.286 ± 0.003 and 0.426 ± 0.002 are obtained for electrons and muons, respectively, where the reported errors are the statistical error on the measurement. The electron prompt and fake rates differ from those of muons because the electron identification and isolation criteria are more stringent than those for muons. The contribution of non-prompt leptons to the total background estimation is presented in Table 1.

The systematic uncertainty in the estimation of backgrounds involving fake leptons is caused by the variations due to the flavor composition of the background (i.e. any dependence of the fake rates on the flavor source of the fake lepton), the level of closure in the method (studied in $\mathrm{t\bar{t}}$ MC events), any potential dependence on kinematic parameters that alter the background composition (such as $H_{\mathrm{T}}^{\mathrm{lep}}$), as well as any potential dependence of the fake rate on η or p_{T}. The uncertaintiy due to these effects is found to be within 50% and hence we assign a 50% systematic uncertainty to the estimation of backgrounds due to fake leptons.

5.2 Event yields

Figure 2 shows the $H_{\mathrm{T}}^{\mathrm{lep}}$ distributions after applying the quarkonia veto, associated Z boson veto, primary Z boson veto, and a requirement of at least two AK4 jets in the event. These distributions are for illustrative purposes only: the full selection is not applied because of the limited number of events. The uncertainty bands in the upper and lower panels of each plot include both statistical and systematic uncertainties.

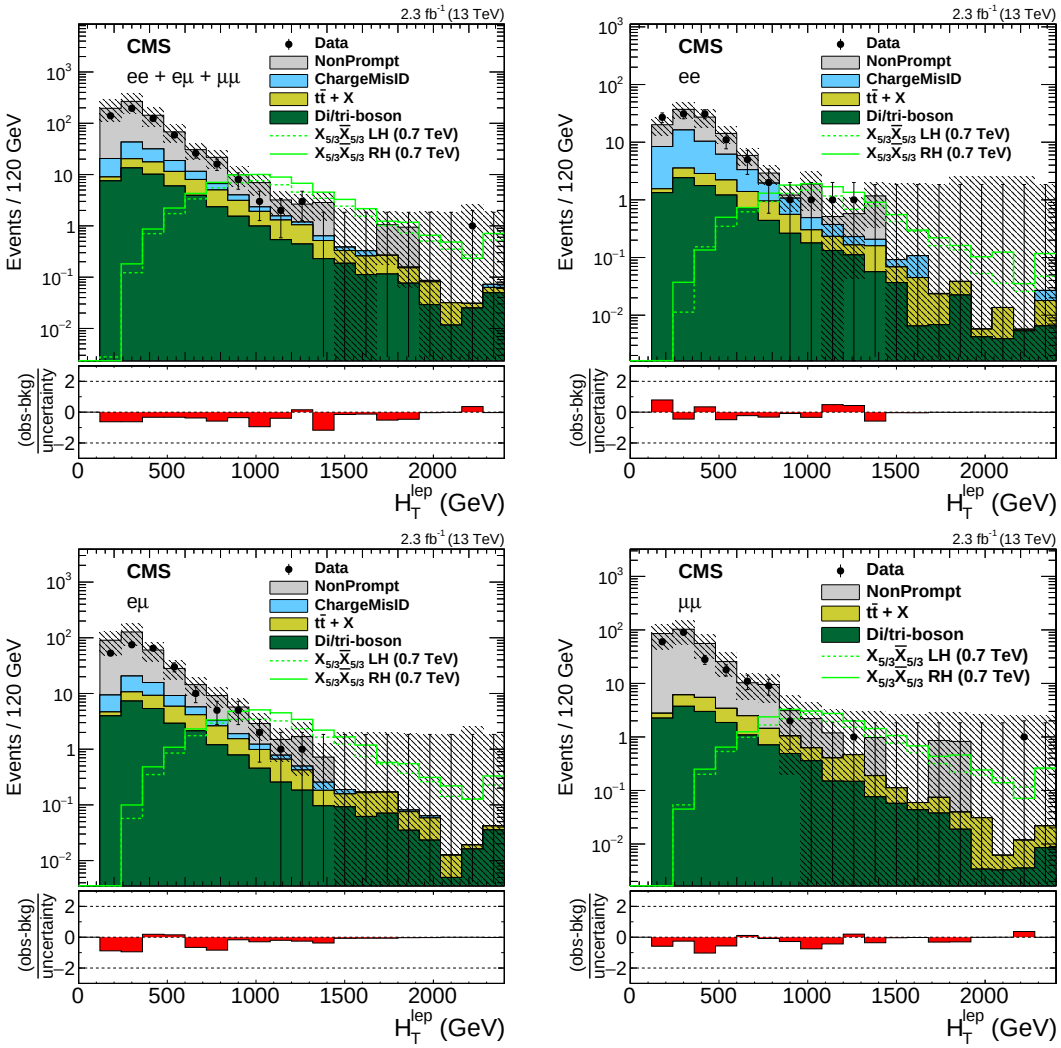

Figure 2: The $H_{\mathrm{T}}^{\mathrm{lep}}$ distributions after the same-sign dilepton selection, Z/quarkonia lepton invariant mass vetoes, and the requirement of at least two AK4 jets in the event. The hatched area shows the combined systematic and statistical uncertainty in the background prediction for each bin. The lower panel in all plots shows the difference between the observed and the predicted numbers of events divided by the total uncertainty. The total uncertainty is calculated as the sum in quadrature of the statistical uncertainty in the observed measurement and the uncertainty in the background, including both statistical and systematic components. Also shown are the distributions for a 700 GeV $X_{5/3}$ with right-handed (solid line) and left-handed (dashed line) couplings to W bosons.

The total number of expected background events are reported in Table 1, together with the numbers of observed and expected events for a right-handed $X_{5/3}$ with a mass of 800 GeV. In total four events are observed, which is consistent with the predicted background, taking its uncertainty into account.

Table 1: Summary of background yields from SM processes with two same-sign prompt leptons (SSP MC), same-sign non-prompt leptons (NonPrompt), and opposite-sign prompt leptons (ChargeMisID), as well as observed data events after the full analysis selection for the same-sign dilepton channel, with an integrated luminosity of 2.3 fb^{-1}. Also shown are the numbers of expected events for a right-handed $X_{5/3}$ with a mass of 800 GeV. The uncertainties include both statistical and systematic components, as discussed in Section 7.

Channel	SSP MC	NonPrompt	ChargeMisID	Total background	800 GeV $X_{5/3}$	Observed
Dielectron	0.7 ± 0.1	1.2 ± 1.0	0.2 ± 0.1	2.1 ± 1.0	3.2 ± 0.3	1
Electron-muon	1.7 ± 0.2	2.6 ± 2.0	0.3 ± 0.1	4.6 ± 2.0	9.1 ± 0.7	1
Dimuon	1.2 ± 0.2	4.6 ± 3.0	0.0 ± 0.0	5.8 ± 3.0	5.6 ± 0.4	2
Total	3.6 ± 0.4	8.4 ± 5.0	0.5 ± 0.2	12.5 ± 5.0	17.9 ± 1.3	4

6 Single-lepton final state

The search for $X_{5/3}$ in the single-lepton final state targets events where one of the W bosons decays into a lepton and a neutrino, while the other three W bosons decay hadronically. The SM background processes leading to a similar final state can be grouped into three categories: top quark, electroweak and QCD multijet backgrounds. The "top quark background" group, labeled "TOP", is dominated by $t\bar{t}$ pair production and also includes single top quark production processes and the rare SM processes $t\bar{t}W$ and $t\bar{t}Z$ (the $t\bar{t}H$ contribution is negligible). The "electroweak background" group, labeled "EWK", is dominated by W+jets production, and includes the DY and diboson (WW, WZ, ZZ) contributions.

A preselection of events is made by requiring exactly one lepton with $p_T > 50$ GeV that also passes the tight identification and isolation requirements described in Section 4. Events containing any additional loose lepton with $p_T > 10$ GeV are ignored.

Because of the significant amount of jet activity in the final state for a potential signal, we require at least three jets, where the p_T of the leading jet is greater than 200 GeV and that of the subleading jet is greater than 90 GeV. To remove the residual multijet events in which jets overlap with the lepton, an additional selection criterion is imposed by requiring that the lepton and the closest jet either be separated by $\Delta R(\ell, \text{closest jet}) > 0.4$, or the magnitude of the lepton p_T perpendicular to the jet axis be larger than 40 GeV. In order to suppress the multijet background contribution, a large missing transverse energy requirement, $E_T^{miss} > 100$ GeV, is imposed.

A discriminant produced by the combined secondary vertex (CSVv2) algorithm [42] is used to identify jets that are likely to have originated from the production of a bottom quark. At the discriminant value used to select b-tagged jets, the algorithm has a single-jet signal efficiency of $\sim$65% and a light quark mistag efficiency of only $\sim$1%. We require at least one of the jets in each event to be b tagged.

Decay products of heavy particles such as $X_{5/3}$ can have large Lorentz boosts, and their subsequent decay products can merge into a single jet. The substructure of these jets is explored using larger-radius jets, reconstructed with an anti-k_t distance parameter of 0.8 (AK8), in order to identify merged jets that are likely to originate from a W boson or a top quark [43]. The "*N*-

subjettiness" [44] algorithm measures the likelihood of a jet having N subjets ($N = 1, 2, 3$, etc). Jet grooming techniques are used to remove soft jet constituents so that the mass of the hard constituents can be measured more precisely. The "pruning" [45] and "soft-drop" [46] algorithms are used to identify boosted hadronic W boson decays and boosted hadronic top quark decays, respectively. The W-tagged jets are required to have $p_T > 200\,\text{GeV}$, $|\eta| < 2.4$, pruned mass between 65 and 105 GeV, and the ratio of N-subjettiness variables [44] $\tau_2/\tau_1 < 0.6$, which ensures that the W-tagged jets are more likely to have two subjets than one subjet. The pruned jet mass scale and resolution, along with the efficiency of the τ_2/τ_1 selection, are compared between data and simulation in a control region dominated by $\bar{t}t$ events with boosted hadronic W boson decays and scale factors are applied in the simulation to match them with the performance found in data. The t-tagged jets are required to have $p_T > 400\,\text{GeV}$, $|\eta| < 2.4$, soft-drop mass between 110 and 210 GeV, and the ratio of N-subjettiness variables $\tau_3/\tau_2 < 0.69$, which ensures that the t-tagged jets are more likely to have three subjets than two subjets. Figure 3 shows the number of AK4 jets, as well as the numbers of t-, W-, and b-tagged jets. The figure also shows that, at this level of the selection, the sample is largely dominated by top quark events, with some contribution from electroweak processes; the contribution from QCD multijet processes is negligible.

In a second step, the selections on the lepton p_T, E_T^{miss}, jet p_T, number of AK4 jets, and on the distance between the lepton and the subleading jet, $\Delta R(\ell, j_2)$, are optimized in a procedure that minimizes the upper limit on the $X_{5/3}$ cross section expected in the absence of a signal. This procedure was also cross checked with an alternative method that maximizes the expected significance and similar selection requirements have been found. The final selection demands, in addition to the preselection requirements listed earlier, the presence of at least four jets, the lepton $p_T > 80\,\text{GeV}$, and $\Delta R(\ell, j_2) > 1$.

The mass constructed from the lepton and b-tagged jet, labeled $M(\ell, b)$, provides good discrimination between signal and background. In case more than one b-tagged jet is found in the event, the one that leads to the smallest $M(\ell, b)$ defines the discriminating variable, $\min[M(\ell, b)]$, which is used in the analysis to extract or constrain the signal. The distribution of $\min[M(\ell, b)]$ is shown in Fig. 4, together with the distance between the lepton and the subleading jet in the event, $\Delta R(\ell, j_2)$, for events passing the final selection criteria, except for the requirement on $\Delta R(\ell, j_2)$. The distribution of $\min[M(\ell, b)]$ for the background, dominated by $\bar{t}t$ events, features a sharp drop around 150 GeV, since, for such events, this variable represents the visible mass of the top quark in the detector. The $\Delta R(\ell, j_2)$ variable shows that the subleading jets populate both the same and opposite hemisphere relative to the lepton in the background events, whereas in the $X_{5/3}$ signal events, the subleading jet is usually opposite to the lepton. This is used in the final selection to further suppress the background contribution in the signal region as well as to reduce the signal contamination in the control region, as discussed in the following section.

6.1 Background modeling

In the single-lepton final state analysis, all the SM background processes are estimated using simulation. To cross check the background modeling, we consider two control regions to study the two dominant background processes in this analysis: one enriched in $\bar{t}t$ events, and the other enriched in W+jets events. In order to define these control regions, events are selected by imposing the same requirements as for the final selection apart from the $\Delta R(\ell, j_2)$ and the b tagging requirements. The selection on $\Delta R(\ell, j_2)$ is inverted, requiring this variable to be less than 1.

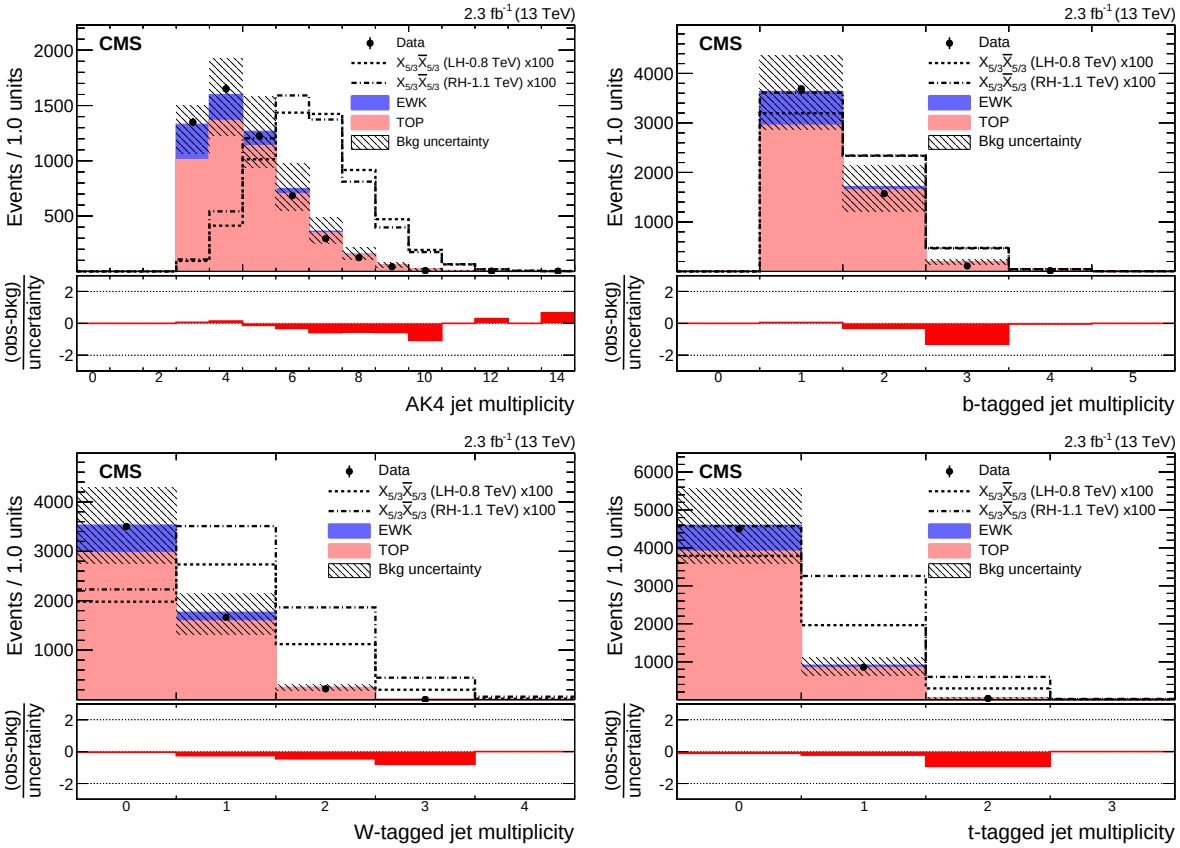

Figure 3: Distributions of the number of AK4 jets (upper left), the numbers of b-tagged (upper right), W-tagged (lower left), and t-tagged jets (lower right) in data and simulation for combined electron and muon event samples, at the preselection level. The lower panel in all plots shows the difference between the observed and the predicted numbers of events divided by the total uncertainty. The total uncertainty is calculated as the sum in quadrature of the statistical uncertainty in the observed measurement and the uncertainty in the background, including both statistical and systematic components. Also shown are the distributions of representative signal events, which are scaled by a factor of 100.

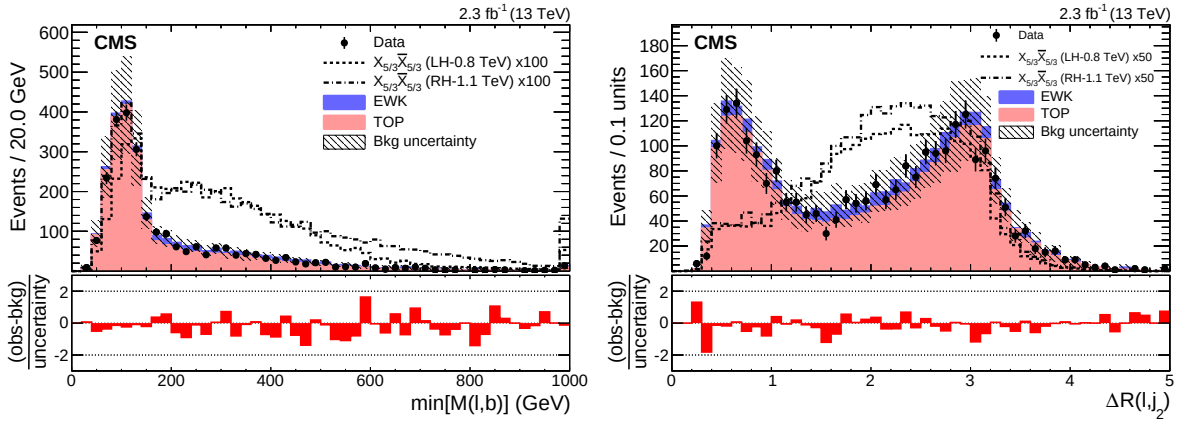

Figure 4: Distributions of min[M(ℓ, b)] (left) and $\Delta R(\ell, j_2)$ (right) in data and simulation for selected events with at least four jets and lepton $p_T > 80$ GeV. The lower panel in all plots shows the difference between the observed and the predicted numbers of events divided by the total uncertainty. The total uncertainty is calculated as the sum in quadrature of the statistical uncertainty in the observed measurement and the uncertainty in the background, including both statistical and systematic components. Also shown are the min[M(ℓ, b)] ($\Delta R(\ell, j_2)$) distributions of representative signal events, which are scaled by a factor of 100 (50) so that the shape differences between signal and background are visible.

The $t\bar{t}$ background control region is then defined by selecting events that have $\geq$1 b-tagged jets, while the W+jets control region is obtained by requiring the presence of 0 b-tagged jets. For the W+jets sample, owing to the 0 b-tagged jet requirement, we use each and every selected jet in the event as a b-jet candidate to obtain the mass discriminant, and denote it as min[M(ℓ, jet)].

In the $t\bar{t}$ control region, the events are split into two categories, one with exactly 1 b-tagged jet, and the other with two or more b-tagged jets. For the W+jets control region, we also define two categories of events, but now based on the number of W-tagged jets: 0 W-tagged, or 1 or more W-tagged jets. Figure 5 shows the min[M(ℓ, b)] (min[M(ℓ, jet)]) distributions in the $t\bar{t}$ (W+jets) control region. The comparison of the observed and the predicted yields in the control regions for each tagging category is used as a closure test for background modeling. In both control regions, the background predictions based on simulation show good agreement with data, and any deviation from unity of the ratio between data and simulation is well within the combined uncertainties.

6.2 Event yields

In order to maximize sensitivity to the presence of a $X_{5/3}$ signal, in the single-lepton final state analysis events are divided into 16 categories based on lepton flavor (e, μ), and the numbers of t-tagged (0, $\geq$1), W-tagged (0, $\geq$1), and b-tagged (1, $\geq$2) jets. Event yields after the final selection are given in Table 2. In Figs. 6 and 7 we show the distributions of min[M(ℓ, b)] after the final selections for events in eight different event categories, depending on the numbers of t-, W-, and b-tagged jets, after combining the electron and muon channels. The observed distributions are well reproduced by the SM predictions in all analysis categories.

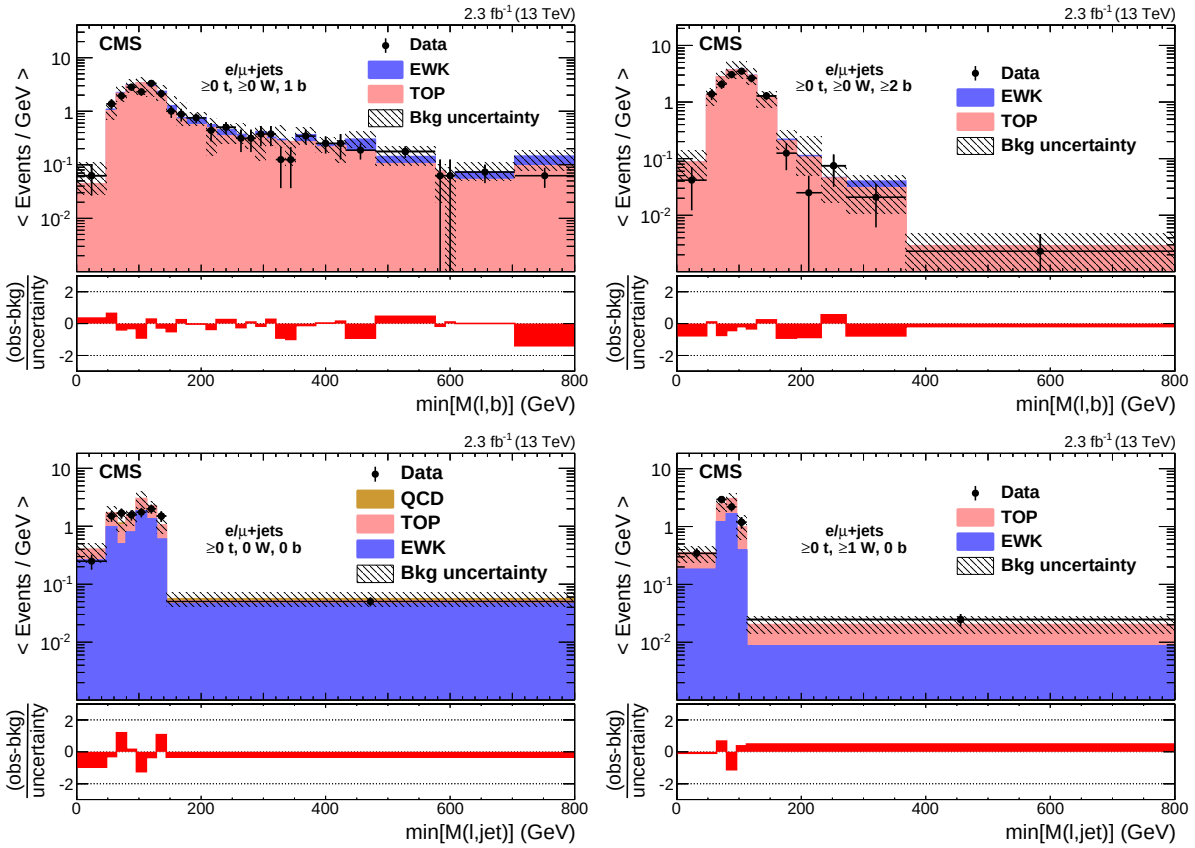

Figure 5: Distributions of min[M(ℓ, b)] in the $\mathrm{t\bar{t}}$ control region, for 1 b-tagged jet (upper left) and $\geq$2 b-tagged jets (upper right) categories, and of min[M(ℓ, jet)] in the W+jets control region, for 0 W-tagged (lower left) and $\geq$1 W-tagged jet (lower right) categories for combined electron and muon event samples. The horizontal bars on the data points indicate the bin widths. The lower panel in all plots shows the difference between the observed and the predicted numbers of events divided by the total uncertainty. The total uncertainty is calculated as the sum in quadrature of the statistical uncertainty in the observed measurement and the uncertainty in the background, including both statistical and systematic components. A small QCD multijet contribution is displayed in the bottom left plot; in all other distributions, it is less than 0.5% and is not shown.

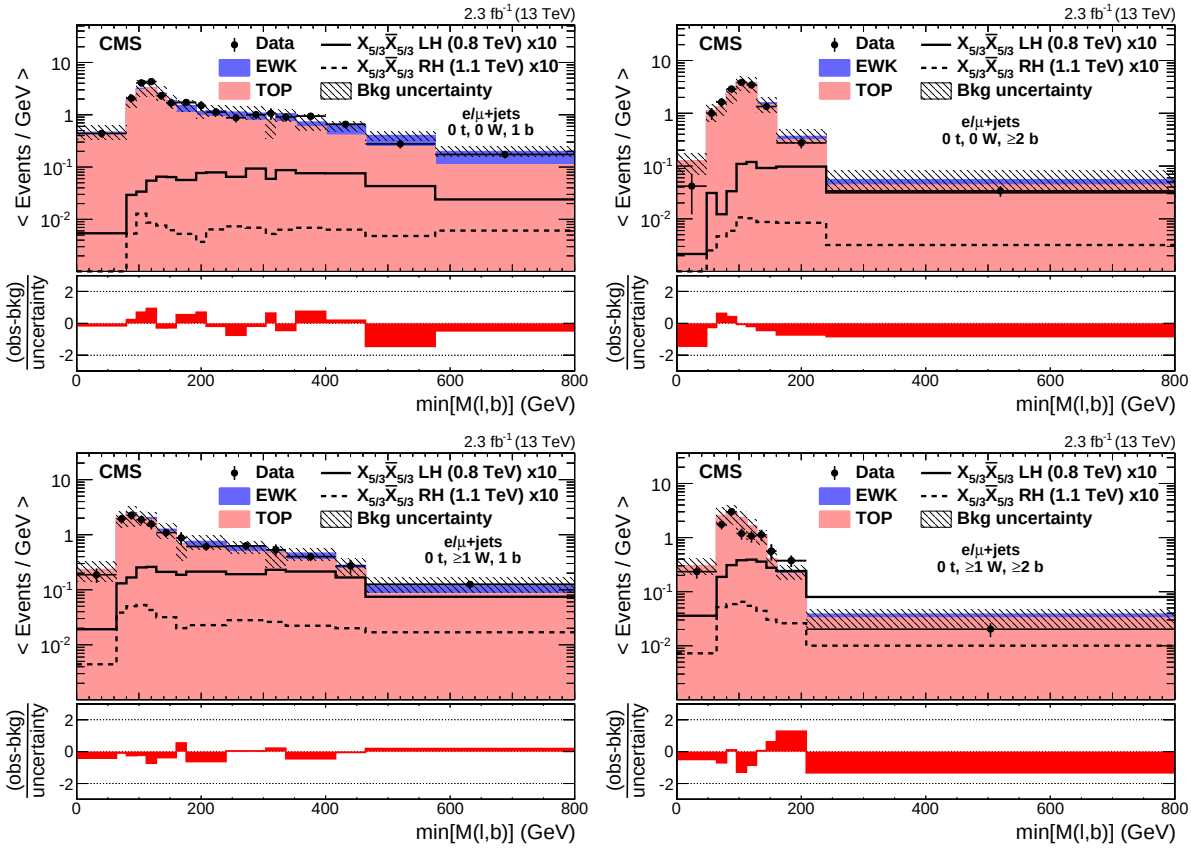

Figure 6: Distributions of min[M(ℓ, b)] in (upper) 0 or (lower) $\geq$1 W-tagged jets and (left) 1 or (right) $\geq$2 b-tagged jets categories with 0 t-tagged jets for combined electron and muon samples, at the final selection level. The horizontal bars on the data points indicate the bin widths. The lower panel in all plots shows the difference between the observed and the predicted numbers of events divided by the total uncertainty. The total uncertainty is calculated as the sum in quadrature of the statistical uncertainty in the observed measurement and the uncertainty in the background, including both statistical and systematic components. Also shown are the distributions of representative signal events, which are scaled by a factor of 10.

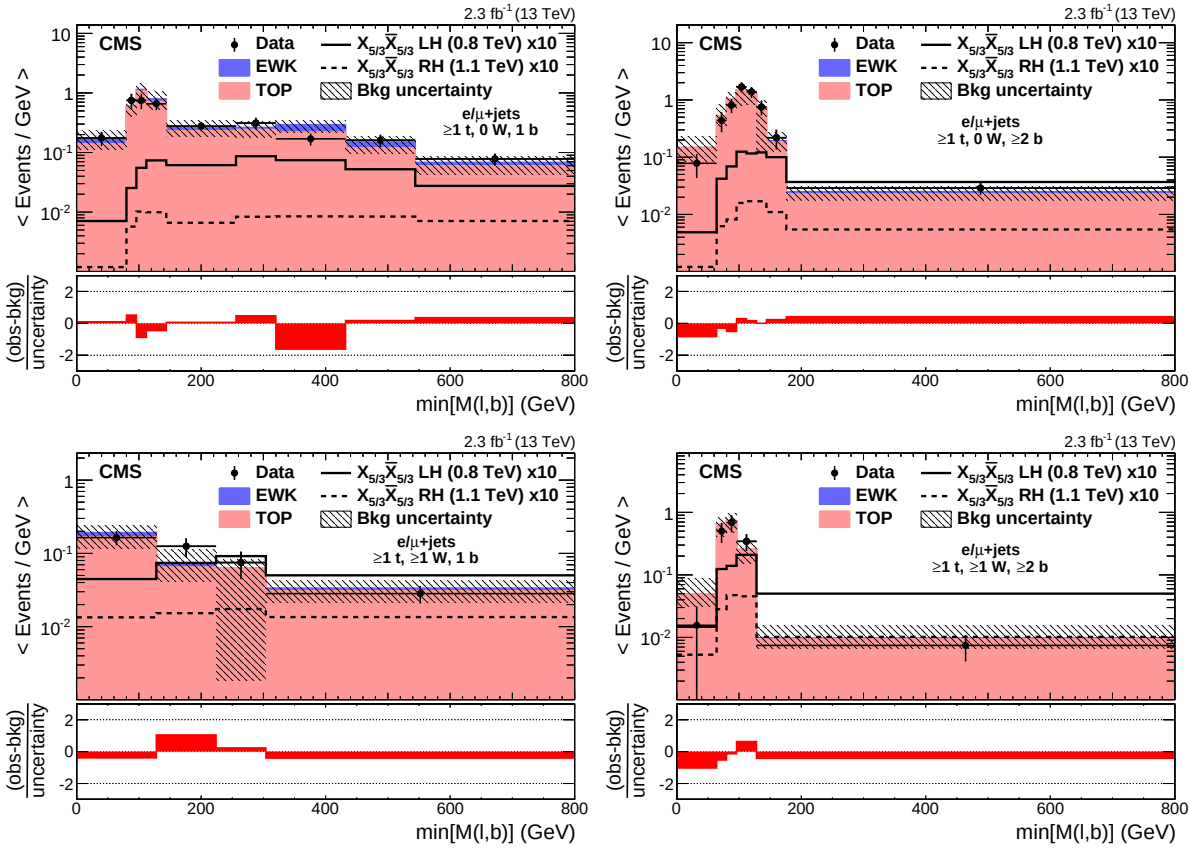

Figure 7: Distributions of min[M(ℓ, b)] in 0 (upper) and $\geq$1 (lower) W-tagged jets and 1 (left) and $\geq$2 (right) b-tagged jets categories with $\geq$1 t-tagged jets for combined electron and muon samples, at the final selection level. The horizontal bars on the data points indicate the bin widths. The lower panel in all plots shows the difference between the observed and the predicted numbers of events divided by the total uncertainty. The total uncertainty is calculated as the sum in quadrature of the statistical uncertainty in the observed measurement and the uncertainty in the background, including both statistical and systematic components. Also shown are the distributions of representative signal events, which are scaled by a factor of 10.

Table 2: Expected (observed) numbers of background (data) events passing the final selection requirements, in the eight tagging categories after combining electron and muon categories, for the single-lepton channel, with an integrated luminosity of 2.3 fb^{-1}. Also shown are the numbers of expected events for an LH $X_{5/3}$ with a mass of 800 GeV and an RH $X_{5/3}$ with a mass of 1.1 TeV. Uncertainties quoted in the table include both statistical as well as the systematic components listed in Table 5. The Poisson uncertainty upper bound (<1.8) is used for the categories where the QCD multijet event yield is zero.

Sample	0 t, 0 W, 1 b	0 t, 0 W, ≥2 b	0 t, ≥1 W, 1 b	0 t, ≥1 W, ≥2 b
LH $X_{5/3}$ (0.8 TeV)	3.75 ± 0.31	3.35 ± 0.35	10.75 ± 0.58	9.16 ± 0.72
RH $X_{5/3}$ (1.1 TeV)	0.453 ± 0.043	0.329 ± 0.039	1.71 ± 0.10	1.25 ± 0.11
TOP	490 ± 140	300 ± 80	342 ± 98	219 ± 64
EWK	132 ± 29	15.4 ± 5.7	53 ± 14	6.6 ± 3.6
QCD	2.1 ± 2.0	<1.8	<1.8	<1.8
Total bkg.	630 ± 140	316 ± 84	395 ± 99	226 ± 64
Data	644	290	366	184

Sample	≥1 t, 0 W, 1 b	≥1 t, 0 W, ≥2 b	≥1 t, ≥1 W, 1 b	≥1 t, ≥1 W, ≥2 b
LH $X_{5/3}$ (0.8 TeV)	3.79 ± 0.28	3.41 ± 0.33	4.51 ± 0.33	4.55 ± 0.41
RH $X_{5/3}$ (1.1 TeV)	0.565 ± 0.046	0.486 ± 0.047	1.128 ± 0.087	0.98 ± 0.10
TOP	155 ± 44	110 ± 32	48 ± 15	40 ± 10
EWK	26.0 ± 8.1	2.3 ± 1.6	5.4 ± 2.9	0.31 ± 0.31
QCD	0.057 ± 0.11	<1.8	<1.8	<1.8
Total bkg.	181 ± 45	113 ± 32	53 ± 16	40 ± 10
Data	167	111	53	36

7 Systematic uncertainties

The principal systematic uncertainties that are common to both analyses are presented in this section, while the uncertainties specific to each analysis are presented in Sections 7.1 and 7.2. The uncertainties in the object selection are derived from uncertainties on the efficiency of the trigger, lepton reconstruction, lepton identification and isolation. These uncertainties are derived from the tag-and-probe studies mentioned in Section 4 and are summarized in Table 3. Lepton identification and isolation uncertainties are applied per lepton, while trigger uncertainties are applied per event. We also include a 2.3% uncertainty in the luminosity measurement [47]. The above uncertainties are applied only to simulation.

Table 3: Details of systematic uncertainties applied for lepton triggering, identification ("ID"), isolation ("ISO"), and integrated luminosity.

Source	Value	Application
Electron ID	1%	per electron
Electron ISO	1%	per electron
Electron trigger	5%	per event
Electron-electron trigger	3%	per event
Muon ID	1%	per muon
Muon ISO	1%	per muon
Muon trigger	5%	per event
Muon-muon trigger	3%	per event
Electron-muon trigger	3%	per event
Integrated luminosity	2.3%	per event

The uncertainties that can affect the shape of the distributions, in particular those related to the jet energy scale (JES) and the jet energy resolution (JER), are assessed by varying the relevant parameters up and down by one standard deviation (s.d.) and repeating the analysis. The PDF uncertainty is evaluated using the complete set of NNPDF 3.0 PDF eigenvectors, following the prescription described in Ref. [48]. The uncertainty due to the renormalization and factorization scales is taken into account by varying the scales up or down by a factor of two and taking the maximum variation. The uncertainty due to the pileup distribution in the simulation is assessed by varying the total inelastic cross section used in the pileup reweighting by $\pm 5\%$.

The theoretical uncertainties due to the factorization and renormalization scales and the PDFs lead to negligible uncertainties in the signal acceptance in the same-sign dilepton channel. The single-lepton channel considers the shape variations in the signal distributions as a result of these uncertainties.

7.1 The same-sign dilepton final state

The uncertainties for simulated events are summarized in Table 4, which includes uncertainties related to jet energy scale, jet energy resolution, pileup, and the overall normalization uncertainty for each simulated background sample. The normalization uncertainty takes into account the uncertainty in the cross section and the uncertainty related to the PDFs used to generate the samples. For the rare backgrounds that have either not been observed, or not well measured, we assume a conservative normalization uncertainty of 50%. We see variations of up to 2% for JER and up to 6% for pileup for some of the simulated background samples. For the signal, the JES, JER, and pileup uncertainties in the acceptance correspond to 5%, 3%, and 1%, respectively.

Table 4: Systematic uncertainties in the same-sign dilepton final state, associated with the simulated processes. The "Normalization" column refers to uncertainties from the cross section normalization and the choice of PDF.

Process	JES	JER	Pileup	Normalization
$t\bar{t}W$	2%	2%	6%	18%
$t\bar{t}Z$	3%	2%	6%	11%
$t\bar{t}H$	4%	2%	6%	12%
$t\bar{t}t\bar{t}$	2%	2%	6%	50%
WZ	10%	2%	6%	12%
ZZ	7%	2%	6%	12%
WW	6%	2%	6%	50%
WWZ	7%	2%	6%	50%
WZZ	9%	2%	6%	50%
ZZZ	9%	2%	6%	50%
$X_{5/3}$	5%	3%	1%	—

As described in Sections 5.1.2 and 5.1.3, we also include a 30% uncertainty for the charge misidentification probability and a 50% uncertainty associated with the estimation of the Non-Prompt background. The latter is the dominant source of uncertainty in the total background prediction.

7.2 The single-lepton final state

The sources of uncertainties in the single-lepton final state are classified according to their effect: having the potential to modify normalizations only, shapes only, or both normalizations and shapes. The uncertainties that affects the normalizations only are listed in Table 3.

To model the uncertainties that alter shapes, we consider uncertainties related to the JES, JER, b tagging and light quark mistagging efficiencies, W tagging uncertainties, t tagging uncertainties, event pileup conditions, PDFs, and renormalization, factorization, and parton shower energy scales. The effect of reweighting the top quark p_T distribution in $t\bar{t}$ events, following the prescription of [49], is considered as a one-sided systematic uncertainty. The $t\bar{t}$ and single top parton shower energy scale uncertainties are assessed by independently varying the scales up and down by a factor of two. A summary of these systematic uncertainties, and how they are applied to signal and background samples is given in Table 5. In the single-lepton channel the uncertainties in the simulated background processes are dominated by the renormalization and factorization scale uncertainties.

Table 5: Summary of all systematic uncertainties considered in the single-lepton channel. Each uncertainty is included in both signal and all background processes unless noted otherwise.

Source	Uncertainty	Comment
Shape and normalization		
JES	±1 s.d. (p_T, η)	
JER	±1 s.d. (η)	
b/c tagging	±1 s.d. (p_T)	
Light quark mistagging	±1 s.d.	
W tagging: mass resolution	±1 s.d. (η)	
W tagging: mass scale	±1 s.d. (p_T, η)	
W tagging: τ_2/τ_1	±1 s.d.	
t tagging	±1 s.d.	
Pileup	$\sigma_{\text{inel.}} \pm 5\%$	
PDF	±1 s.d.	Only for background
Renorm./fact. energy scale	Envelope ($\times2$, $\times0.5$)	Only for background
Parton shower scale	Envelope ($\times2$, $\times0.5$)	Only for $t\bar{t}$ and single top
Top quark p_T	Δ (weighted, nominal)	Only for $t\bar{t}$
Shape only		
PDF	±1 s.d.	Only for signal
Renorm./fact. energy scale	Envelope ($\times2$, $\times0.5$)	Only for signal

8 Results

We find no significant excess in the data compared to the SM expectations and therefore proceed to set 95% CL upper limits on the production cross section for $pp \to X_{5/3}\overline{X}_{5/3} \to tW^+\bar{t}W^-$. Expected and observed limits are calculated using Bayesian statistics [50] with a flat prior distribution in the signal cross section, for both LH and RH $X_{5/3}$ scenarios. The same-sign dilepton analysis uses a counting experiment to derive limits based on the full set of requirements detailed above, while the single-lepton channel uses a binned likelihood fit to the distribution of the min[M(ℓ, b)] variable. Systematic uncertainties are represented as nuisance parameters with log-normal priors for normalization uncertainties, Gaussian priors for shape uncertainties with results obtained via the maximum-likelihood value on the signal cross section. Using the full set of analysis selection criteria and an integrated luminosity of 2.3 fb^{-1}, we obtain observed (expected) limits of 1000 (890) GeV for an RH $X_{5/3}$ and 970 (860) GeV for an LH $X_{5/3}$ at 95% CL in the same-sign dilepton channel. Using the single-lepton channel, the observed (expected) limits are found to be 770 (780) GeV for an RH $X_{5/3}$ and 800 (780) GeV for an LH $X_{5/3}$, again at 95% CL. Both the expected and the observed limits after combining all categories in each signature are shown in Fig. 8, where the PDF, and renormalization and factorization scale uncertainties in the signal cross section are shown as the band around the theoretical predic-

tions. The observed limit being consistently lower than the expected limit for the same-sign dilepton results in figure 8 is simply due to the analysis requirements being independent of signal mass.

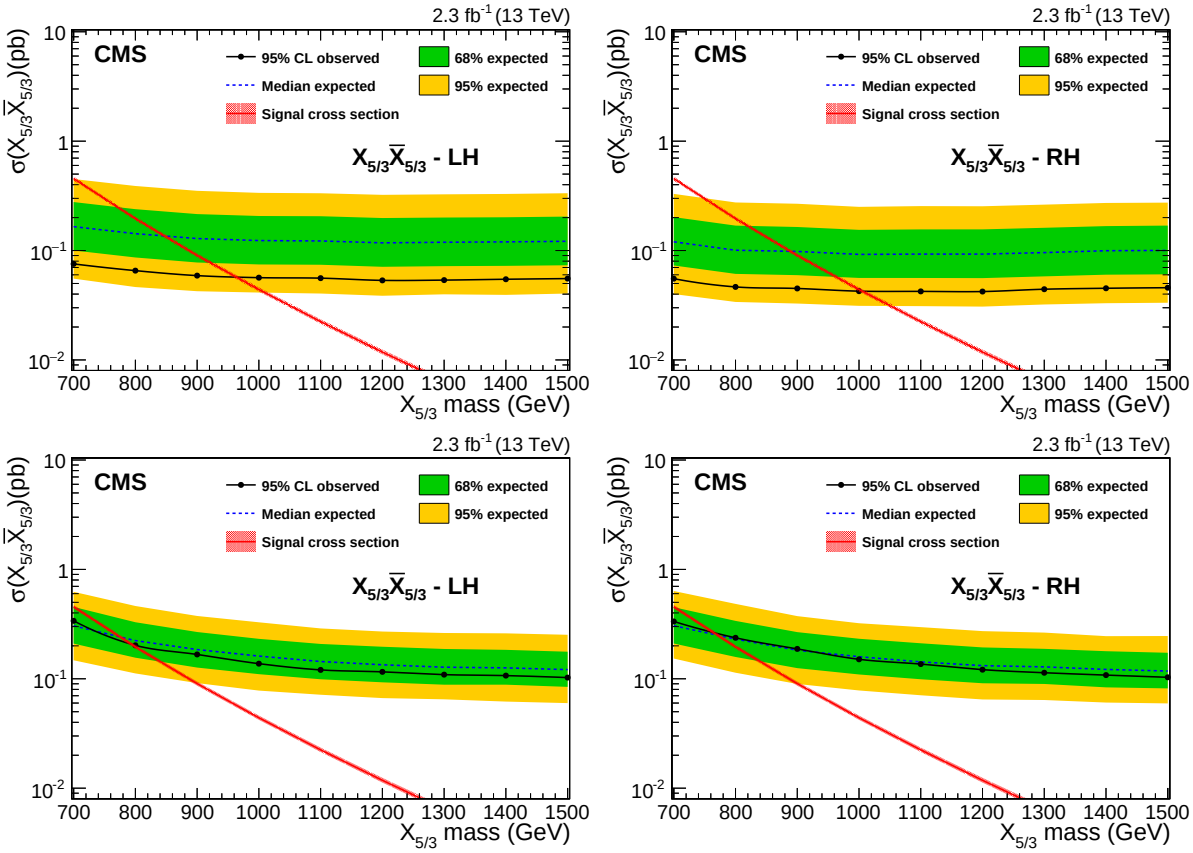

Figure 8: The expected and observed upper limits at 95% CL for a left-handed (left) and right-handed (right) $X_{5/3}$ for the same-sign dilepton signature (upper) and the single-lepton signature (lower) after combining all channels in each signature. The theoretical prediction for the $X_{5/3}$ pair production cross section is shown as a band including its uncertainty.

A combination of the results from the analyses of the two final states discussed in this paper, same-sign dilepton and the single-lepton signatures, is shown in Fig. 9. In the combination, the observed (expected) exclusion limit on the mass of an RH $X_{5/3}$ is found to be 1020 (910) GeV. For the LH $X_{5/3}$ signal, the observed (expected) lower limit on the mass is 990 (890) GeV.

9 Summary

A search has been performed for the production of heavy partners of the top quark with charge 5/3 decaying into a top quark and a W boson, using 2.3 fb^{-1} of proton-proton collision data collected by the CMS experiment at 13 TeV. Events with two different signatures are analyzed: final states with either a pair of same-sign leptons or a single lepton, along with jets. No significant excess is observed in the data above the expected standard model background. Upper bounds at 95% confidence level are set on the production cross section of heavy top quark partners. The $X_{5/3}$ masses with right-handed (left-handed) couplings below 1020 (990) GeV are excluded at 95% confidence level. These are the most stringent limits placed on the $X_{5/3}$ mass and the first limits based on a combination of these two different final states.

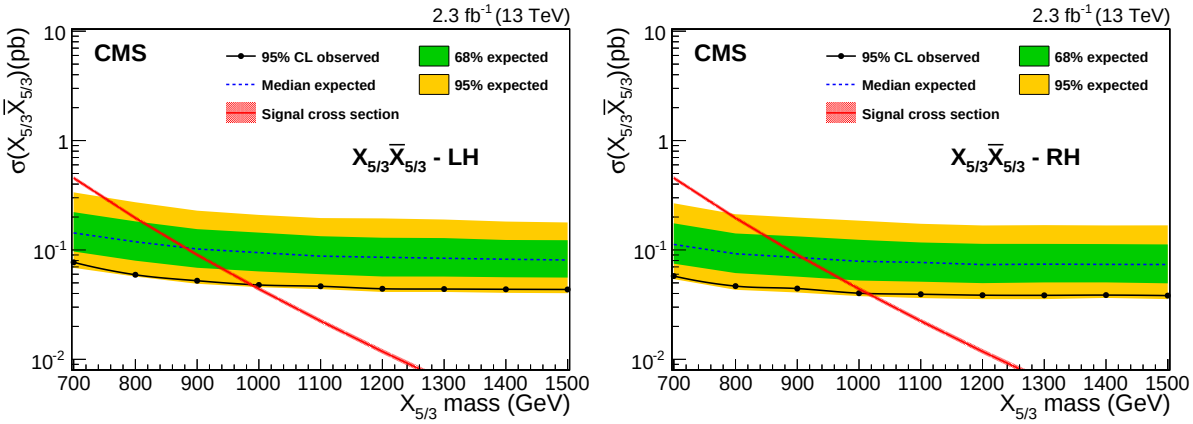

Figure 9: The expected and observed upper limits at 95% CL after combining the same-sign dilepton and the single-lepton signatures for left-handed (left) and right-handed (right) $X_{5/3}$ scenarios. The theoretical prediction for the $X_{5/3}$ pair production cross section is shown as a band including its uncertainty.

Acknowledgments

We congratulate our colleagues in the CERN accelerator departments for the excellent performance of the LHC and thank the technical and administrative staffs at CERN and at other CMS institutes for their contributions to the success of the CMS effort. In addition, we gratefully acknowledge the computing centres and personnel of the Worldwide LHC Computing Grid for delivering so effectively the computing infrastructure essential to our analyses. Finally, we acknowledge the enduring support for the construction and operation of the LHC and the CMS detector provided by the following funding agencies: BMWFW and FWF (Austria); FNRS and FWO (Belgium); CNPq, CAPES, FAPERJ, and FAPESP (Brazil); MES (Bulgaria); CERN; CAS, MoST, and NSFC (China); COLCIENCIAS (Colombia); MSES and CSF (Croatia); RPF (Cyprus); SENESCYT (Ecuador); MoER, ERC IUT, and ERDF (Estonia); Academy of Finland, MEC, and HIP (Finland); CEA and CNRS/IN2P3 (France); BMBF, DFG, and HGF (Germany); GSRT (Greece); OTKA and NIH (Hungary); DAE and DST (India); IPM (Iran); SFI (Ireland); INFN (Italy); MSIP and NRF (Republic of Korea); LAS (Lithuania); MOE and UM (Malaysia); BUAP, CINVESTAV, CONACYT, LNS, SEP, and UASLP-FAI (Mexico); MBIE (New Zealand); PAEC (Pakistan); MSHE and NSC (Poland); FCT (Portugal); JINR (Dubna); MON, RosAtom, RAS, RFBR and RAEP (Russia); MESTD (Serbia); SEIDI, CPAN, PCTI and FEDER (Spain); Swiss Funding Agencies (Switzerland); MST (Taipei); ThEPCenter, IPST, STAR, and NSTDA (Thailand); TUBITAK and TAEK (Turkey); NASU and SFFR (Ukraine); STFC (United Kingdom); DOE and NSF (USA).

Individuals have received support from the Marie-Curie programme and the European Research Council and Horizon 2020 Grant, contract No. 675440 (European Union); the Leventis Foundation; the A. P. Sloan Foundation; the Alexander von Humboldt Foundation; the Belgian Federal Science Policy Office; the Fonds pour la Formation à la Recherche dans l'Industrie et dans l'Agriculture (FRIA-Belgium); the Agentschap voor Innovatie door Wetenschap en Technologie (IWT-Belgium); the Ministry of Education, Youth and Sports (MEYS) of the Czech Republic; the Council of Science and Industrial Research, India; the HOMING PLUS programme of the Foundation for Polish Science, cofinanced from European Union, Regional Development Fund, the Mobility Plus programme of the Ministry of Science and Higher Education, the National Science Center (Poland), contracts Harmonia 2014/14/M/ST2/00428,

Opus 2014/13/B/ST2/02543, 2014/15/B/ST2/03998, and 2015/19/B/ST2/02861, Sonata-bis 2012/07/E/ST2/01406; the National Priorities Research Program by Qatar National Research Fund; the Programa Clarín-COFUND del Principado de Asturias; the Thalis and Aristeia programmes cofinanced by EU-ESF and the Greek NSRF; the Rachadapisek Sompot Fund for Postdoctoral Fellowship, Chulalongkorn University and the Chulalongkorn Academic into Its 2nd Century Project Advancement Project (Thailand); and the Welch Foundation, contract C-1845.

References

[1] A. De Simone, O. Matsedonskyi, R. Rattazzi, and A. Wulzer, "A first top partner hunter's guide", *JHEP* **04** (2013) 004, doi:10.1007/JHEP04(2013)004, arXiv:1211.5663.

[2] J. Mrazek and A. Wulzer, "A strong sector at the LHC: Top partners in same-sign dileptons", *Phys. Rev. D* **81** (2010) 075006, doi:10.1103/PhysRevD.81.075006, arXiv:0909.3977.

[3] G. Dissertori, E. Furlan, F. Moortgat, and P. Nef, "Discovery potential of top-partners in a realistic composite Higgs model with early LHC data", *JHEP* **09** (2010) 019, doi:10.1007/JHEP09(2010)019, arXiv:1005.4414.

[4] R. Contino and G. Servant, "Discovering the top partners at the LHC using same-sign dilepton final states", *JHEP* **06** (2008) 026, doi:10.1088/1126-6708/2008/06/026, arXiv:0801.1679.

[5] A. Azatov and J. Galloway, "Light custodians and Higgs physics in composite models", *Phys. Rev. D* **85** (2012) 055013, doi:10.1103/PhysRevD.85.055013, arXiv:1110.5646.

[6] CMS Collaboration, "Search for top-quark partners with charge 5/3 in the same-sign dilepton final state", *Phys. Rev. Lett.* **112** (2014) 171801, doi:10.1103/PhysRevLett.112.171801, arXiv:1312.2391.

[7] ATLAS Collaboration, "Analysis of events with b-jets and a pair of leptons of the same charge in pp collisions at $\sqrt{s} = 8$ TeV with the ATLAS detector", *JHEP* **10** (2015) 150, doi:10.1007/JHEP10(2015)150, arXiv:1504.04605.

[8] ATLAS Collaboration, "Search for vector-like B quarks in events with one isolated lepton, missing transverse momentum and jets at $\sqrt{s} = 8$ TeV with the ATLAS detector", *Phys. Rev. D* **91** (2015) 112011, doi:10.1103/PhysRevD.91.112011, arXiv:1503.05425.

[9] CMS Collaboration, "The CMS experiment at the CERN LHC", *JINST* **3** (2008) S08004, doi:10.1088/1748-0221/3/08/S08004.

[10] J. Alwall et al., "The automated computation of tree-level and next-to-leading order differential cross sections, and their matching to parton shower simulations", *JHEP* **07** (2014) 079, doi:10.1007/JHEP07(2014)079, arXiv:1405.0301.

[11] P. Artoisenet, R. Frederix, O. Mattelaer, and R. Rietkerk, "Automatic spin-entangled decays of heavy resonances in Monte Carlo simulations", *JHEP* **03** (2013) 015, doi:10.1007/JHEP03(2013)015, arXiv:1212.3460.

[12] M. Czakon and A. Mitov, "Top++: A program for the calculation of the top-pair cross-section at hadron colliders", *Comput. Phys. Commun.* **185** (2014) 2930, doi:10.1016/j.cpc.2014.06.021.

[13] M. Czakon, P. Fiedler, and A. Mitov, "Total top-quark pair-production cross section at hadron colliders through $\mathcal{O}(\alpha_S^4)$", *Phys. Rev. Lett.* **110** (2013) 252004, doi:10.1103/PhysRevLett.110.252004.

[14] M. Czakon and A. Mitov, "NNLO corrections to top pair production at hadron colliders: the quark-gluon reaction", *JHEP* **01** (2013) 080, doi:10.1007/JHEP01(2013)080.

[15] M. Czakon and A. Mitov, "NNLO corrections to top-pair production at hadron colliders: the all-fermionic scattering channels", *JHEP* **12** (2012) 054, doi:10.1007/JHEP12(2012)054.

[16] P. Bärnreuther, M. Czakon, and A. Mitov, "Percent-level-precision physics at the Tevatron: Next-to-next-to-leading order QCD corrections to $q\bar{q} \to t\bar{t} + X$", *Phys. Rev. Lett.* **109** (2012) 132001, doi:10.1103/PhysRevLett.109.132001, arXiv:1204.5201.

[17] M. Cacciari et al., "Top-pair production at hadron colliders with next-to-next-to-leading logarithmic soft-gluon resummation", *Phys. Lett. B* **710** (2012) 612, doi:10.1016/j.physletb.2012.03.013.

[18] J. Alwall et al., "Comparative study of various algorithms for the merging of parton showers and matrix elements in hadronic collisions", *Eur. Phys. J. C* **53** (2008) 473, doi:10.1140/epjc/s10052-007-0490-5, arXiv:0706.2569.

[19] R. Frederix and S. Frixione, "Merging meets matching in MC@NLO", *JHEP* **12** (2012) 061, doi:10.1007/JHEP12(2012)061, arXiv:1209.6215.

[20] P. Nason, "A new method for combining NLO QCD with shower Monte Carlo algorithms", *JHEP* **11** (2004) 040, doi:10.1088/1126-6708/2004/11/040, arXiv:hep-ph/0409146.

[21] S. Frixione, P. Nason, and C. Oleari, "Matching NLO QCD computations with parton shower simulations: the POWHEG method", *JHEP* **11** (2007) 070, doi:10.1088/1126-6708/2007/11/070, arXiv:0709.2092.

[22] S. Alioli, P. Nason, C. Oleari, and E. Re, "A general framework for implementing NLO calculations in shower Monte Carlo programs: the POWHEG BOX", *JHEP* **06** (2010) 043, doi:10.1007/JHEP06(2010)043, arXiv:1002.2581.

[23] S. Alioli, S.-O. Moch, and P. Uwer, "Hadronic top-quark pair-production with one jet and parton showering", *JHEP* **01** (2012) 137, doi:10.1007/JHEP01(2012)137, arXiv:1110.5251.

[24] T. Sjöstrand, S. Mrenna, and P. Z. Skands, "A brief introduction to PYTHIA 8.1", *Comput. Phys. Commun.* **178** (2008) 852, doi:10.1016/j.cpc.2008.01.036, arXiv:0710.3820.

[25] T. Sjöstrand et al., "An introduction to PYTHIA 8.2", *Comput. Phys. Commun.* **191** (2015) 159, doi:10.1016/j.cpc.2015.01.024, arXiv:1410.3012.

[26] NNPDF Collaboration, "Parton distributions for the LHC Run II", *JHEP* **04** (2015) 040, doi:10.1007/JHEP04(2015)040, arXiv:1410.8849.

[27] P. Skands, S. Carrazza, and J. Rojo, "Tuning PYTHIA 8.1: the Monash 2013 tune", *Eur. Phys. J. C* **74** (2014) 3024, doi:10.1140/epjc/s10052-014-3024-y, arXiv:1404.5630.

[28] GEANT4 Collaboration, "GEANT4—a simulation toolkit", *Nucl. Instrum. Meth. A* **506** (2003) 250, doi:10.1016/S0168-9002(03)01368-8.

[29] J. Allison et al., "Geant4 developments and applications", *IEEE Trans. Nucl. Sci.* **53** (2006) 270, doi:10.1109/TNS.2006.869826.

[30] CMS Collaboration, "Particle-flow reconstruction and global event description with the CMS detector", (2017). arXiv:1706.04965. Submitted to *JINST*.

[31] CMS Collaboration, "Performance of electron reconstruction and selection with the CMS detector in proton-proton collisions at $\sqrt{s} = 8$ TeV", *JINST* **10** (2015) P06005, doi:10.1088/1748-0221/10/06/P06005, arXiv:1502.02701.

[32] CMS Collaboration, "Description and performance of track and primary-vertex reconstruction with the CMS tracker", *JINST* **9** (2014) P10009, doi:10.1088/1748-0221/9/10/P10009, arXiv:1405.6569.

[33] W. Adam, R. Frühwirth, A. Strandlie, and T. Todorov, "Reconstruction of electrons with the Gaussian-sum filter in the CMS tracker at LHC", *J. Phys G* **31** (2005) N9, doi:10.1088/0954-3899/31/9/N01, arXiv:physics/0306087.

[34] M. Cacciari and G. P. Salam, "Pileup subtraction using jet areas", *Phys. Lett. B* **659** (2008) 119, doi:10.1016/j.physletb.2007.09.077, arXiv:0707.1378.

[35] CMS Collaboration, "Measurement of the inclusive W and Z production cross sections in pp collisions at $\sqrt{s} = 7$ TeV", *JHEP* **10** (2011) 132, doi:10.1007/JHEP10(2011)132, arXiv:1107.4789.

[36] M. Cacciari, G. P. Salam, and G. Soyez, "The anti-k_t jet clustering algorithm", *JHEP* **04** (2008) 063, doi:10.1088/1126-6708/2008/04/063, arXiv:0802.1189.

[37] M. Cacciari, G. P. Salam, and G. Soyez, "The catchment area of jets", *JHEP* **04** (2008) 005, doi:10.1088/1126-6708/2008/04/005, arXiv:0802.1188.

[38] M. Cacciari, G. P. Salam, and G. Soyez, "FastJet user manual", *Eur. Phys. J. C* **72** (2012) 1896, doi:10.1140/epjc/s10052-012-1896-2, arXiv:1111.6097.

[39] CMS Collaboration, "Jet energy scale and resolution in the CMS experiment in pp collisions at 8 TeV", *JINST* **12** (2017) P02014, doi:10.1088/1748-0221/12/02/P02014, arXiv:1607.03663.

[40] CMS Collaboration, "Search for new physics in same-sign dilepton events in proton-proton collisions at $\sqrt{s} = 13$ TeV", *Eur. Phys. J. C* **76** (2016) 439, doi:10.1140/epjc/s10052-016-4261-z, arXiv:1605.03171.

[41] CMS Collaboration, "Search for new physics with same-sign isolated dilepton events with jets and missing transverse energy at the LHC", *JHEP* **06** (2011) 077, doi:10.1007/JHEP06(2011)077, arXiv:1104.3168.

[42] CMS Collaboration, "Identification of b quark jets at the CMS experiment in the LHC Run 2", CMS Physics Analysis Summary CMS-PAS-BTV-15-001, 2016.

[43] CMS Collaboration, "Top tagging with new approaches", CMS Physics Analysis Summary CMS-PAS-JME-15-002, 2016.

[44] J. Thaler and K. Van Tilburg, "Maximizing boosted top identification by minimizing N-subjettiness", *JHEP* **02** (2012) 093, doi:10.1007/JHEP02(2012)093, arXiv:1108.2701.

[45] S. D. Ellis, C. K. Vermilion, and J. R. Walsh, "Techniques for improved heavy particle searches with jet substructure", *Phys. Rev. D* **80** (2009) 051501, doi:10.1103/PhysRevD.80.051501, arXiv:0903.5081.

[46] A. J. Larkoski, S. Marzani, G. Soyez, and J. Thaler, "Soft drop", *JHEP* **05** (2014) 146, doi:10.1007/JHEP05(2014)146, arXiv:1402.2657.

[47] CMS Collaboration, "CMS luminosity measurement for the 2015 data-taking period", CMS Physics Analysis Summary CMS-PAS-LUM-15-001, 2017.

[48] J. Butterworth et al., "PDF4LHC recommendations for LHC Run II", *J. Phys. G* **43** (2016) 023001, doi:10.1088/0954-3899/43/2/023001, arXiv:1510.03865.

[49] CMS Collaboration, "Measurement of the differential cross section for top quark pair production in pp collisions at $\sqrt{s} = 8$ TeV", *Eur. Phys. J. C* **75** (2015) 542, doi:10.1140/epjc/s10052-015-3709-x, arXiv:1505.04480.

[50] T. Müller, J. Ott, and J. Wagner-Kuhr, "Theta—a framework for template-based modeling and inference", (2010). http://www-ekp.physik.uni-karlsruhe.de/~ott/theta/testing/html/index.html.

A The CMS Collaboration

Yerevan Physics Institute, Yerevan, Armenia
A.M. Sirunyan, A. Tumasyan

Institut für Hochenergiephysik, Wien, Austria
W. Adam, E. Asilar, T. Bergauer, J. Brandstetter, E. Brondolin, M. Dragicevic, J. Erö, M. Flechl, M. Friedl, R. Frühwirth[1], V.M. Ghete, C. Hartl, N. Hörmann, J. Hrubec, M. Jeitler[1], A. König, I. Krätschmer, D. Liko, T. Matsushita, I. Mikulec, D. Rabady, N. Rad, B. Rahbaran, H. Rohringer, J. Schieck[1], J. Strauss, W. Waltenberger, C.-E. Wulz[1]

Institute for Nuclear Problems, Minsk, Belarus
V. Chekhovsky, V. Mossolov, J. Suarez Gonzalez

National Centre for Particle and High Energy Physics, Minsk, Belarus
N. Shumeiko

Universiteit Antwerpen, Antwerpen, Belgium
S. Alderweireldt, E.A. De Wolf, X. Janssen, J. Lauwers, M. Van De Klundert, H. Van Haevermaet, P. Van Mechelen, N. Van Remortel, A. Van Spilbeeck

Vrije Universiteit Brussel, Brussel, Belgium
S. Abu Zeid, F. Blekman, J. D'Hondt, I. De Bruyn, J. De Clercq, K. Deroover, S. Lowette, S. Moortgat, L. Moreels, A. Olbrechts, Q. Python, K. Skovpen, S. Tavernier, W. Van Doninck, P. Van Mulders, I. Van Parijs

Université Libre de Bruxelles, Bruxelles, Belgium
H. Brun, B. Clerbaux, G. De Lentdecker, H. Delannoy, G. Fasanella, L. Favart, R. Goldouzian, A. Grebenyuk, G. Karapostoli, T. Lenzi, J. Luetic, T. Maerschalk, A. Marinov, A. Randle-conde, T. Seva, C. Vander Velde, P. Vanlaer, D. Vannerom, R. Yonamine, F. Zenoni, F. Zhang[2]

Ghent University, Ghent, Belgium
A. Cimmino, T. Cornelis, D. Dobur, A. Fagot, M. Gul, I. Khvastunov, D. Poyraz, S. Salva, R. Schöfbeck, M. Tytgat, W. Van Driessche, W. Verbeke, N. Zaganidis

Université Catholique de Louvain, Louvain-la-Neuve, Belgium
H. Bakhshiansohi, O. Bondu, S. Brochet, G. Bruno, A. Caudron, S. De Visscher, C. Delaere, M. Delcourt, B. Francois, A. Giammanco, A. Jafari, M. Komm, G. Krintiras, V. Lemaitre, A. Magitteri, A. Mertens, M. Musich, K. Piotrzkowski, L. Quertenmont, M. Vidal Marono, S. Wertz

Université de Mons, Mons, Belgium
N. Beliy

Centro Brasileiro de Pesquisas Fisicas, Rio de Janeiro, Brazil
W.L. Aldá Júnior, F.L. Alves, G.A. Alves, L. Brito, C. Hensel, A. Moraes, M.E. Pol, P. Rebello Teles

Universidade do Estado do Rio de Janeiro, Rio de Janeiro, Brazil
E. Belchior Batista Das Chagas, W. Carvalho, J. Chinellato[3], A. Custódio, E.M. Da Costa, G.G. Da Silveira[4], D. De Jesus Damiao, S. Fonseca De Souza, L.M. Huertas Guativa, H. Malbouisson, C. Mora Herrera, L. Mundim, H. Nogima, A. Santoro, A. Sznajder, E.J. Tonelli Manganote[3], F. Torres Da Silva De Araujo, A. Vilela Pereira

Universidade Estadual Paulista [a], Universidade Federal do ABC [b], São Paulo, Brazil
S. Ahuja[a], C.A. Bernardes[a], T.R. Fernandez Perez Tomei[a], E.M. Gregores[b], P.G. Mercadante[b], C.S. Moon[a], S.F. Novaes[a], Sandra S. Padula[a], D. Romero Abad[b], J.C. Ruiz Vargas[a]

Institute for Nuclear Research and Nuclear Energy, Sofia, Bulgaria
A. Aleksandrov, R. Hadjiiska, P. Iaydjiev, M. Rodozov, S. Stoykova, G. Sultanov, M. Vutova

University of Sofia, Sofia, Bulgaria
A. Dimitrov, I. Glushkov, L. Litov, B. Pavlov, P. Petkov

Beihang University, Beijing, China
W. Fang[5], X. Gao[5]

Institute of High Energy Physics, Beijing, China
M. Ahmad, J.G. Bian, G.M. Chen, H.S. Chen, M. Chen, Y. Chen, C.H. Jiang, D. Leggat, Z. Liu, F. Romeo, S.M. Shaheen, A. Spiezia, J. Tao, C. Wang, Z. Wang, E. Yazgan, H. Zhang, J. Zhao

State Key Laboratory of Nuclear Physics and Technology, Peking University, Beijing, China
Y. Ban, G. Chen, Q. Li, S. Liu, Y. Mao, S.J. Qian, D. Wang, Z. Xu

Universidad de Los Andes, Bogota, Colombia
C. Avila, A. Cabrera, L.F. Chaparro Sierra, C. Florez, J.P. Gomez, C.F. González Hernández, J.D. Ruiz Alvarez

University of Split, Faculty of Electrical Engineering, Mechanical Engineering and Naval Architecture, Split, Croatia
N. Godinovic, D. Lelas, I. Puljak, P.M. Ribeiro Cipriano, T. Sculac

University of Split, Faculty of Science, Split, Croatia
Z. Antunovic, M. Kovac

Institute Rudjer Boskovic, Zagreb, Croatia
V. Brigljevic, D. Ferencek, K. Kadija, B. Mesic, T. Susa

University of Cyprus, Nicosia, Cyprus
M.W. Ather, A. Attikis, G. Mavromanolakis, J. Mousa, C. Nicolaou, F. Ptochos, P.A. Razis, H. Rykaczewski

Charles University, Prague, Czech Republic
M. Finger[6], M. Finger Jr.[6]

Universidad San Francisco de Quito, Quito, Ecuador
E. Carrera Jarrin

Academy of Scientific Research and Technology of the Arab Republic of Egypt, Egyptian Network of High Energy Physics, Cairo, Egypt
A.A. Abdelalim[7,8], Y. Mohammed[9], E. Salama[10,11]

National Institute of Chemical Physics and Biophysics, Tallinn, Estonia
R.K. Dewanjee, M. Kadastik, L. Perrini, M. Raidal, A. Tiko, C. Veelken

Department of Physics, University of Helsinki, Helsinki, Finland
P. Eerola, J. Pekkanen, M. Voutilainen

Helsinki Institute of Physics, Helsinki, Finland
J. Härkönen, T. Järvinen, V. Karimäki, R. Kinnunen, T. Lampén, K. Lassila-Perini, S. Lehti, T. Lindén, P. Luukka, E. Tuominen, J. Tuominiemi, E. Tuovinen

Lappeenranta University of Technology, Lappeenranta, Finland
J. Talvitie, T. Tuuva

IRFU, CEA, Université Paris-Saclay, Gif-sur-Yvette, France
M. Besancon, F. Couderc, M. Dejardin, D. Denegri, J.L. Faure, F. Ferri, S. Ganjour, S. Ghosh, A. Givernaud, P. Gras, G. Hamel de Monchenault, P. Jarry, I. Kucher, E. Locci, M. Machet, J. Malcles, J. Rander, A. Rosowsky, M.Ö. Sahin, M. Titov

Laboratoire Leprince-Ringuet, Ecole polytechnique, CNRS/IN2P3, Université Paris-Saclay, Palaiseau, France
A. Abdulsalam, I. Antropov, S. Baffioni, F. Beaudette, P. Busson, L. Cadamuro, E. Chapon, C. Charlot, O. Davignon, R. Granier de Cassagnac, M. Jo, S. Lisniak, A. Lobanov, P. Miné, M. Nguyen, C. Ochando, G. Ortona, P. Paganini, P. Pigard, S. Regnard, R. Salerno, Y. Sirois, A.G. Stahl Leiton, T. Strebler, Y. Yilmaz, A. Zabi, A. Zghiche

Université de Strasbourg, CNRS, IPHC UMR 7178, F-67000 Strasbourg, France
J.-L. Agram[12], J. Andrea, D. Bloch, J.-M. Brom, M. Buttignol, E.C. Chabert, N. Chanon, C. Collard, E. Conte[12], X. Coubez, J.-C. Fontaine[12], D. Gelé, U. Goerlach, A.-C. Le Bihan, P. Van Hove

Centre de Calcul de l'Institut National de Physique Nucleaire et de Physique des Particules, CNRS/IN2P3, Villeurbanne, France
S. Gadrat

Université de Lyon, Université Claude Bernard Lyon 1, CNRS-IN2P3, Institut de Physique Nucléaire de Lyon, Villeurbanne, France
S. Beauceron, C. Bernet, G. Boudoul, R. Chierici, D. Contardo, B. Courbon, P. Depasse, H. El Mamouni, J. Fay, L. Finco, S. Gascon, M. Gouzevitch, G. Grenier, B. Ille, F. Lagarde, I.B. Laktineh, M. Lethuillier, L. Mirabito, A.L. Pequegnot, S. Perries, A. Popov[13], V. Sordini, M. Vander Donckt, S. Viret

Georgian Technical University, Tbilisi, Georgia
A. Khvedelidze[6]

Tbilisi State University, Tbilisi, Georgia
L. Rurua

RWTH Aachen University, I. Physikalisches Institut, Aachen, Germany
C. Autermann, S. Beranek, L. Feld, M.K. Kiesel, K. Klein, M. Lipinski, M. Preuten, C. Schomakers, J. Schulz, T. Verlage

RWTH Aachen University, III. Physikalisches Institut A, Aachen, Germany
A. Albert, M. Brodski, E. Dietz-Laursonn, D. Duchardt, M. Endres, M. Erdmann, S. Erdweg, T. Esch, R. Fischer, A. Güth, M. Hamer, T. Hebbeker, C. Heidemann, K. Hoepfner, S. Knutzen, M. Merschmeyer, A. Meyer, P. Millet, S. Mukherjee, M. Olschewski, K. Padeken, T. Pook, M. Radziej, H. Reithler, M. Rieger, F. Scheuch, L. Sonnenschein, D. Teyssier, S. Thüer

RWTH Aachen University, III. Physikalisches Institut B, Aachen, Germany
G. Flügge, B. Kargoll, T. Kress, A. Künsken, J. Lingemann, T. Müller, A. Nehrkorn, A. Nowack, C. Pistone, O. Pooth, A. Stahl[14]

Deutsches Elektronen-Synchrotron, Hamburg, Germany
M. Aldaya Martin, T. Arndt, C. Asawatangtrakuldee, K. Beernaert, O. Behnke, U. Behrens, A.A. Bin Anuar, K. Borras[15], V. Botta, A. Campbell, P. Connor, C. Contreras-Campana, F. Costanza, C. Diez Pardos, G. Eckerlin, D. Eckstein, T. Eichhorn, E. Eren, E. Gallo[16],

J. Garay Garcia, A. Geiser, A. Gizhko, J.M. Grados Luyando, A. Grohsjean, P. Gunnellini, A. Harb, J. Hauk, M. Hempel[17], H. Jung, A. Kalogeropoulos, O. Karacheban[17], M. Kasemann, J. Keaveney, C. Kleinwort, I. Korol, D. Krücker, W. Lange, A. Lelek, T. Lenz, J. Leonard, K. Lipka, W. Lohmann[17], R. Mankel, I.-A. Melzer-Pellmann, A.B. Meyer, G. Mittag, J. Mnich, A. Mussgiller, E. Ntomari, D. Pitzl, R. Placakyte, A. Raspereza, B. Roland, M. Savitskyi, P. Saxena, R. Shevchenko, S. Spannagel, N. Stefaniuk, G.P. Van Onsem, R. Walsh, Y. Wen, K. Wichmann, C. Wissing

University of Hamburg, Hamburg, Germany
S. Bein, V. Blobel, M. Centis Vignali, A.R. Draeger, T. Dreyer, E. Garutti, D. Gonzalez, J. Haller, M. Hoffmann, A. Junkes, R. Klanner, R. Kogler, N. Kovalchuk, S. Kurz, T. Lapsien, I. Marchesini, D. Marconi, M. Meyer, M. Niedziela, D. Nowatschin, F. Pantaleo[14], T. Peiffer, A. Perieanu, C. Scharf, P. Schleper, A. Schmidt, S. Schumann, J. Schwandt, J. Sonneveld, H. Stadie, G. Steinbrück, F.M. Stober, M. Stöver, H. Tholen, D. Troendle, E. Usai, L. Vanelderen, A. Vanhoefer, B. Vormwald

Institut für Experimentelle Kernphysik, Karlsruhe, Germany
M. Akbiyik, C. Barth, S. Baur, C. Baus, J. Berger, E. Butz, R. Caspart, T. Chwalek, F. Colombo, W. De Boer, A. Dierlamm, B. Freund, R. Friese, M. Giffels, A. Gilbert, D. Haitz, F. Hartmann[14], S.M. Heindl, U. Husemann, F. Kassel[14], S. Kudella, H. Mildner, M.U. Mozer, Th. Müller, M. Plagge, G. Quast, K. Rabbertz, M. Schröder, I. Shvetsov, G. Sieber, H.J. Simonis, R. Ulrich, S. Wayand, M. Weber, T. Weiler, S. Williamson, C. Wöhrmann, R. Wolf

Institute of Nuclear and Particle Physics (INPP), NCSR Demokritos, Aghia Paraskevi, Greece
G. Anagnostou, G. Daskalakis, T. Geralis, V.A. Giakoumopoulou, A. Kyriakis, D. Loukas, I. Topsis-Giotis

National and Kapodistrian University of Athens, Athens, Greece
S. Kesisoglou, A. Panagiotou, N. Saoulidou

University of Ioánnina, Ioánnina, Greece
I. Evangelou, G. Flouris, C. Foudas, P. Kokkas, N. Manthos, I. Papadopoulos, E. Paradas, J. Strologas, F.A. Triantis

MTA-ELTE Lendület CMS Particle and Nuclear Physics Group, Eötvös Loránd University, Budapest, Hungary
M. Csanad, N. Filipovic, G. Pasztor

Wigner Research Centre for Physics, Budapest, Hungary
G. Bencze, C. Hajdu, D. Horvath[18], F. Sikler, V. Veszpremi, G. Vesztergombi[19], A.J. Zsigmond

Institute of Nuclear Research ATOMKI, Debrecen, Hungary
N. Beni, S. Czellar, J. Karancsi[20], A. Makovec, J. Molnar, Z. Szillasi

Institute of Physics, University of Debrecen, Debrecen, Hungary
M. Bartók[19], P. Raics, Z.L. Trocsanyi, B. Ujvari

Indian Institute of Science (IISc), Bangalore, India
S. Choudhury, J.R. Komaragiri

National Institute of Science Education and Research, Bhubaneswar, India
S. Bahinipati[21], S. Bhowmik, P. Mal, K. Mandal, A. Nayak[22], D.K. Sahoo[21], N. Sahoo, S.K. Swain

Panjab University, Chandigarh, India
S. Bansal, S.B. Beri, V. Bhatnagar, U. Bhawandeep, R. Chawla, N. Dhingra, A.K. Kalsi, A. Kaur, M. Kaur, R. Kumar, P. Kumari, A. Mehta, M. Mittal, J.B. Singh, G. Walia

University of Delhi, Delhi, India
Ashok Kumar, Aashaq Shah, A. Bhardwaj, S. Chauhan, B.C. Choudhary, R.B. Garg, S. Keshri, S. Malhotra, M. Naimuddin, K. Ranjan, R. Sharma, V. Sharma

Saha Institute of Nuclear Physics, HBNI, Kolkata, India
R. Bhattacharya, S. Bhattacharya, S. Dey, S. Dutt, S. Dutta, S. Ghosh, N. Majumdar, A. Modak, K. Mondal, S. Mukhopadhyay, S. Nandan, A. Purohit, A. Roy, D. Roy, S. Roy Chowdhury, S. Sarkar, M. Sharan, S. Thakur

Indian Institute of Technology Madras, Madras, India
P.K. Behera

Bhabha Atomic Research Centre, Mumbai, India
R. Chudasama, D. Dutta, V. Jha, V. Kumar, A.K. Mohanty[14], P.K. Netrakanti, L.M. Pant, P. Shukla, A. Topkar

Tata Institute of Fundamental Research-A, Mumbai, India
T. Aziz, S. Dugad, B. Mahakud, S. Mitra, G.B. Mohanty, B. Parida, N. Sur, B. Sutar

Tata Institute of Fundamental Research-B, Mumbai, India
S. Banerjee, S. Bhattacharya, S. Chatterjee, P. Das, M. Guchait, Sa. Jain, S. Kumar, M. Maity[23], G. Majumder, K. Mazumdar, T. Sarkar[23], N. Wickramage[24]

Indian Institute of Science Education and Research (IISER), Pune, India
S. Chauhan, S. Dube, V. Hegde, A. Kapoor, K. Kothekar, S. Pandey, A. Rane, S. Sharma

Institute for Research in Fundamental Sciences (IPM), Tehran, Iran
S. Chenarani[25], E. Eskandari Tadavani, S.M. Etesami[25], M. Khakzad, M. Mohammadi Najafabadi, M. Naseri, S. Paktinat Mehdiabadi[26], F. Rezaei Hosseinabadi, B. Safarzadeh[27], M. Zeinali

University College Dublin, Dublin, Ireland
M. Felcini, M. Grunewald

INFN Sezione di Bari [a], Università di Bari [b], Politecnico di Bari [c], Bari, Italy
M. Abbrescia[a,b], C. Calabria[a,b], C. Caputo[a,b], A. Colaleo[a], D. Creanza[a,c], L. Cristella[a,b], N. De Filippis[a,c], M. De Palma[a,b], L. Fiore[a], G. Iaselli[a,c], G. Maggi[a,c], M. Maggi[a], G. Miniello[a,b], S. My[a,b], S. Nuzzo[a,b], A. Pompili[a,b], G. Pugliese[a,c], R. Radogna[a,b], A. Ranieri[a], G. Selvaggi[a,b], A. Sharma[a], L. Silvestris[a,14], R. Venditti[a], P. Verwilligen[a]

INFN Sezione di Bologna [a], Università di Bologna [b], Bologna, Italy
G. Abbiendi[a], C. Battilana, D. Bonacorsi[a,b], S. Braibant-Giacomelli[a,b], L. Brigliadori[a,b], R. Campanini[a,b], P. Capiluppi[a,b], A. Castro[a,b], F.R. Cavallo[a], S.S. Chhibra[a,b], M. Cuffiani[a,b], G.M. Dallavalle[a], F. Fabbri[a], A. Fanfani[a,b], D. Fasanella[a,b], P. Giacomelli[a], L. Guiducci[a,b], S. Marcellini[a], G. Masetti[a], F.L. Navarria[a,b], A. Perrotta[a], A.M. Rossi[a,b], T. Rovelli[a,b], G.P. Siroli[a,b], N. Tosi[a,b,14]

INFN Sezione di Catania [a], Università di Catania [b], Catania, Italy
S. Albergo[a,b], S. Costa[a,b], A. Di Mattia[a], F. Giordano[a,b], R. Potenza[a,b], A. Tricomi[a,b], C. Tuve[a,b]

INFN Sezione di Firenze [a], Università di Firenze [b], Firenze, Italy
G. Barbagli[a], K. Chatterjee[a,b], V. Ciulli[a,b], C. Civinini[a], R. D'Alessandro[a,b], E. Focardi[a,b], P. Lenzi[a,b], M. Meschini[a], S. Paoletti[a], L. Russo[a,28], G. Sguazzoni[a], D. Strom[a], L. Viliani[a,b,14]

INFN Laboratori Nazionali di Frascati, Frascati, Italy
L. Benussi, S. Bianco, F. Fabbri, D. Piccolo, F. Primavera[14]

INFN Sezione di Genova [a], Università di Genova [b], Genova, Italy
V. Calvelli[a,b], F. Ferro[a], M.R. Monge[a,b], E. Robutti[a], S. Tosi[a,b]

INFN Sezione di Milano-Bicocca [a], Università di Milano-Bicocca [b], Milano, Italy
L. Brianza[a,b,14], F. Brivio[a,b], V. Ciriolo, M.E. Dinardo[a,b], S. Fiorendi[a,b,14], S. Gennai[a], A. Ghezzi[a,b], P. Govoni[a,b], M. Malberti[a,b], S. Malvezzi[a], R.A. Manzoni[a,b], D. Menasce[a], L. Moroni[a], M. Paganoni[a,b], K. Pauwels, D. Pedrini[a], S. Pigazzini[a,b], S. Ragazzi[a,b], T. Tabarelli de Fatis[a,b]

INFN Sezione di Napoli [a], Università di Napoli 'Federico II' [b], Napoli, Italy, Università della Basilicata [c], Potenza, Italy, Università G. Marconi [d], Roma, Italy
S. Buontempo[a], N. Cavallo[a,c], S. Di Guida[a,d,14], F. Fabozzi[a,c], F. Fienga[a,b], A.O.M. Iorio[a,b], W.A. Khan[a], L. Lista[a], S. Meola[a,d,14], P. Paolucci[a,14], C. Sciacca[a,b], F. Thyssen[a]

INFN Sezione di Padova [a], Università di Padova [b], Padova, Italy, Università di Trento [c], Trento, Italy
P. Azzi[a,14], N. Bacchetta[a], L. Benato[a,b], D. Bisello[a,b], A. Boletti[a,b], A. Carvalho Antunes De Oliveira[a,b], P. Checchia[a], M. Dall'Osso[a,b], P. De Castro Manzano[a], T. Dorigo[a], U. Dosselli[a], F. Gasparini[a,b], U. Gasparini[a,b], F. Gonella[a], A. Gozzelino[a], S. Lacaprara[a], M. Margoni[a,b], A.T. Meneguzzo[a,b], N. Pozzobon[a,b], P. Ronchese[a,b], R. Rossin[a,b], F. Simonetto[a,b], E. Torassa[a], S. Ventura[a], M. Zanetti[a,b], P. Zotto[a,b]

INFN Sezione di Pavia [a], Università di Pavia [b], Pavia, Italy
A. Braghieri[a], F. Fallavollita[a,b], A. Magnani[a,b], P. Montagna[a,b], S.P. Ratti[a,b], V. Re[a], M. Ressegotti, C. Riccardi[a,b], P. Salvini[a], I. Vai[a,b], P. Vitulo[a,b]

INFN Sezione di Perugia [a], Università di Perugia [b], Perugia, Italy
L. Alunni Solestizi[a,b], G.M. Bilei[a], D. Ciangottini[a,b], L. Fanò[a,b], P. Lariccia[a,b], R. Leonardi[a,b], G. Mantovani[a,b], V. Mariani[a,b], M. Menichelli[a], A. Saha[a], A. Santocchia[a,b], D. Spiga

INFN Sezione di Pisa [a], Università di Pisa [b], Scuola Normale Superiore di Pisa [c], Pisa, Italy
K. Androsov[a], P. Azzurri[a,14], G. Bagliesi[a], J. Bernardini[a], T. Boccali[a], L. Borrello, R. Castaldi[a], M.A. Ciocci[a,b], R. Dell'Orso[a], G. Fedi[a], A. Giassi[a], M.T. Grippo[a,28], F. Ligabue[a,c], T. Lomtadze[a], L. Martini[a,b], A. Messineo[a,b], F. Palla[a], A. Rizzi[a,b], A. Savoy-Navarro[a,29], P. Spagnolo[a], R. Tenchini[a], G. Tonelli[a,b], A. Venturi[a], P.G. Verdini[a]

INFN Sezione di Roma [a], Sapienza Università di Roma [b], Rome, Italy
L. Barone[a,b], F. Cavallari[a], M. Cipriani[a,b], D. Del Re[a,b,14], M. Diemoz[a], S. Gelli[a,b], E. Longo[a,b], F. Margaroli[a,b], B. Marzocchi[a,b], P. Meridiani[a], G. Organtini[a,b], R. Paramatti[a,b], F. Preiato[a,b], S. Rahatlou[a,b], C. Rovelli[a], F. Santanastasio[a,b]

INFN Sezione di Torino [a], Università di Torino [b], Torino, Italy, Università del Piemonte Orientale [c], Novara, Italy
N. Amapane[a,b], R. Arcidiacono[a,c,14], S. Argiro[a,b], M. Arneodo[a,c], N. Bartosik[a], R. Bellan[a,b], C. Biino[a], N. Cartiglia[a], F. Cenna[a,b], M. Costa[a,b], R. Covarelli[a,b], A. Degano[a,b], N. Demaria[a], B. Kiani[a,b], C. Mariotti[a], S. Maselli[a], E. Migliore[a,b], V. Monaco[a,b], E. Monteil[a,b], M. Monteno[a], M.M. Obertino[a,b], L. Pacher[a,b], N. Pastrone[a], M. Pelliccioni[a], G.L. Pinna Angioni[a,b], F. Ravera[a,b],

A. Romero[a,b], M. Ruspa[a,c], R. Sacchi[a,b], K. Shchelina[a,b], V. Sola[a], A. Solano[a,b], A. Staiano[a], P. Traczyk[a,b]

INFN Sezione di Trieste [a], Università di Trieste [b], Trieste, Italy
S. Belforte[a], M. Casarsa[a], F. Cossutti[a], G. Della Ricca[a,b], A. Zanetti[a]

Kyungpook National University, Daegu, Korea
D.H. Kim, G.N. Kim, M.S. Kim, J. Lee, S. Lee, S.W. Lee, Y.D. Oh, S. Sekmen, D.C. Son, Y.C. Yang

Chonbuk National University, Jeonju, Korea
A. Lee

Chonnam National University, Institute for Universe and Elementary Particles, Kwangju, Korea
H. Kim, D.H. Moon

Hanyang University, Seoul, Korea
J.A. Brochero Cifuentes, J. Goh, T.J. Kim

Korea University, Seoul, Korea
S. Cho, S. Choi, Y. Go, D. Gyun, S. Ha, B. Hong, Y. Jo, Y. Kim, K. Lee, K.S. Lee, S. Lee, J. Lim, S.K. Park, Y. Roh

Seoul National University, Seoul, Korea
J. Almond, J. Kim, H. Lee, S.B. Oh, B.C. Radburn-Smith, S.h. Seo, U.K. Yang, H.D. Yoo, G.B. Yu

University of Seoul, Seoul, Korea
M. Choi, H. Kim, J.H. Kim, J.S.H. Lee, I.C. Park, G. Ryu

Sungkyunkwan University, Suwon, Korea
Y. Choi, C. Hwang, J. Lee, I. Yu

Vilnius University, Vilnius, Lithuania
V. Dudenas, A. Juodagalvis, J. Vaitkus

National Centre for Particle Physics, Universiti Malaya, Kuala Lumpur, Malaysia
I. Ahmed, Z.A. Ibrahim, M.A.B. Md Ali[30], F. Mohamad Idris[31], W.A.T. Wan Abdullah, M.N. Yusli, Z. Zolkapli

Centro de Investigacion y de Estudios Avanzados del IPN, Mexico City, Mexico
H. Castilla-Valdez, E. De La Cruz-Burelo, I. Heredia-De La Cruz[32], R. Lopez-Fernandez, J. Mejia Guisao, A. Sanchez-Hernandez

Universidad Iberoamericana, Mexico City, Mexico
S. Carrillo Moreno, C. Oropeza Barrera, F. Vazquez Valencia

Benemerita Universidad Autonoma de Puebla, Puebla, Mexico
I. Pedraza, H.A. Salazar Ibarguen, C. Uribe Estrada

Universidad Autónoma de San Luis Potosí, San Luis Potosí, Mexico
A. Morelos Pineda

University of Auckland, Auckland, New Zealand
D. Krofcheck

University of Canterbury, Christchurch, New Zealand
P.H. Butler

National Centre for Physics, Quaid-I-Azam University, Islamabad, Pakistan
A. Ahmad, M. Ahmad, Q. Hassan, H.R. Hoorani, A. Saddique, M.A. Shah, M. Shoaib, M. Waqas

National Centre for Nuclear Research, Swierk, Poland
H. Bialkowska, M. Bluj, B. Boimska, T. Frueboes, M. Górski, M. Kazana, K. Nawrocki, K. Romanowska-Rybinska, M. Szleper, P. Zalewski

Institute of Experimental Physics, Faculty of Physics, University of Warsaw, Warsaw, Poland
K. Bunkowski, A. Byszuk[33], K. Doroba, A. Kalinowski, M. Konecki, J. Krolikowski, M. Misiura, M. Olszewski, A. Pyskir, M. Walczak

Laboratório de Instrumentação e Física Experimental de Partículas, Lisboa, Portugal
P. Bargassa, C. Beirão Da Cruz E Silva, B. Calpas, A. Di Francesco, P. Faccioli, M. Gallinaro, J. Hollar, N. Leonardo, L. Lloret Iglesias, M.V. Nemallapudi, J. Seixas, O. Toldaiev, D. Vadruccio, J. Varela

Joint Institute for Nuclear Research, Dubna, Russia
S. Afanasiev, P. Bunin, M. Gavrilenko, I. Golutvin, I. Gorbunov, A. Kamenev, V. Karjavin, A. Lanev, A. Malakhov, V. Matveev[34,35], V. Palichik, V. Perelygin, S. Shmatov, S. Shulha, N. Skatchkov, V. Smirnov, N. Voytishin, A. Zarubin

Petersburg Nuclear Physics Institute, Gatchina (St. Petersburg), Russia
Y. Ivanov, V. Kim[36], E. Kuznetsova[37], P. Levchenko, V. Murzin, V. Oreshkin, I. Smirnov, V. Sulimov, L. Uvarov, S. Vavilov, A. Vorobyev

Institute for Nuclear Research, Moscow, Russia
Yu. Andreev, A. Dermenev, S. Gninenko, N. Golubev, A. Karneyeu, M. Kirsanov, N. Krasnikov, A. Pashenkov, D. Tlisov, A. Toropin

Institute for Theoretical and Experimental Physics, Moscow, Russia
V. Epshteyn, V. Gavrilov, N. Lychkovskaya, V. Popov, I. Pozdnyakov, G. Safronov, A. Spiridonov, M. Toms, E. Vlasov, A. Zhokin

Moscow Institute of Physics and Technology, Moscow, Russia
T. Aushev, A. Bylinkin[35]

National Research Nuclear University 'Moscow Engineering Physics Institute' (MEPhI), Moscow, Russia
R. Chistov[38], M. Danilov[38], V. Rusinov

P.N. Lebedev Physical Institute, Moscow, Russia
V. Andreev, M. Azarkin[35], I. Dremin[35], M. Kirakosyan, A. Terkulov

Skobeltsyn Institute of Nuclear Physics, Lomonosov Moscow State University, Moscow, Russia
A. Baskakov, A. Belyaev, E. Boos, M. Dubinin[39], L. Dudko, A. Ershov, A. Gribushin, V. Klyukhin, O. Kodolova, I. Lokhtin, I. Miagkov, S. Obraztsov, S. Petrushanko, V. Savrin, A. Snigirev

Novosibirsk State University (NSU), Novosibirsk, Russia
V. Blinov[40], Y.Skovpen[40], D. Shtol[40]

State Research Center of Russian Federation, Institute for High Energy Physics, Protvino, Russia
I. Azhgirey, I. Bayshev, S. Bitioukov, D. Elumakhov, V. Kachanov, A. Kalinin, D. Konstantinov, V. Krychkine, V. Petrov, R. Ryutin, A. Sobol, S. Troshin, N. Tyurin, A. Uzunian, A. Volkov

University of Belgrade, Faculty of Physics and Vinca Institute of Nuclear Sciences, Belgrade, Serbia
P. Adzic[41], P. Cirkovic, D. Devetak, M. Dordevic, J. Milosevic, V. Rekovic

Centro de Investigaciones Energéticas Medioambientales y Tecnológicas (CIEMAT), Madrid, Spain
J. Alcaraz Maestre, M. Barrio Luna, M. Cerrada, N. Colino, B. De La Cruz, A. Delgado Peris, A. Escalante Del Valle, C. Fernandez Bedoya, J.P. Fernández Ramos, J. Flix, M.C. Fouz, P. Garcia-Abia, O. Gonzalez Lopez, S. Goy Lopez, J.M. Hernandez, M.I. Josa, A. Pérez-Calero Yzquierdo, J. Puerta Pelayo, A. Quintario Olmeda, I. Redondo, L. Romero, M.S. Soares

Universidad Autónoma de Madrid, Madrid, Spain
J.F. de Trocóniz, M. Missiroli, D. Moran

Universidad de Oviedo, Oviedo, Spain
J. Cuevas, C. Erice, J. Fernandez Menendez, I. Gonzalez Caballero, J.R. González Fernández, E. Palencia Cortezon, S. Sanchez Cruz, I. Suárez Andrés, P. Vischia, J.M. Vizan Garcia

Instituto de Física de Cantabria (IFCA), CSIC-Universidad de Cantabria, Santander, Spain
I.J. Cabrillo, A. Calderon, B. Chazin Quero, E. Curras, M. Fernandez, J. Garcia-Ferrero, G. Gomez, A. Lopez Virto, J. Marco, C. Martinez Rivero, F. Matorras, J. Piedra Gomez, T. Rodrigo, A. Ruiz-Jimeno, L. Scodellaro, N. Trevisani, I. Vila, R. Vilar Cortabitarte

CERN, European Organization for Nuclear Research, Geneva, Switzerland
D. Abbaneo, E. Auffray, P. Baillon, A.H. Ball, D. Barney, M. Bianco, P. Bloch, A. Bocci, C. Botta, T. Camporesi, R. Castello, M. Cepeda, G. Cerminara, Y. Chen, D. d'Enterria, A. Dabrowski, V. Daponte, A. David, M. De Gruttola, A. De Roeck, E. Di Marco[42], M. Dobson, B. Dorney, T. du Pree, M. Dünser, N. Dupont, A. Elliott-Peisert, P. Everaerts, G. Franzoni, J. Fulcher, W. Funk, D. Gigi, K. Gill, F. Glege, D. Gulhan, S. Gundacker, M. Guthoff, P. Harris, J. Hegeman, V. Innocente, P. Janot, J. Kieseler, H. Kirschenmann, V. Knünz, A. Kornmayer[14], M.J. Kortelainen, C. Lange, P. Lecoq, C. Lourenço, M.T. Lucchini, L. Malgeri, M. Mannelli, A. Martelli, F. Meijers, J.A. Merlin, S. Mersi, E. Meschi, P. Milenovic[43], F. Moortgat, M. Mulders, H. Neugebauer, S. Orfanelli, L. Orsini, L. Pape, E. Perez, M. Peruzzi, A. Petrilli, G. Petrucciani, A. Pfeiffer, M. Pierini, A. Racz, T. Reis, G. Rolandi[44], M. Rovere, H. Sakulin, J.B. Sauvan, C. Schäfer, C. Schwick, M. Seidel, A. Sharma, P. Silva, P. Sphicas[45], J. Steggemann, M. Stoye, M. Tosi, D. Treille, A. Triossi, A. Tsirou, V. Veckalns[46], G.I. Veres[19], M. Verweij, N. Wardle, A. Zagozdzinska[33], W.D. Zeuner

Paul Scherrer Institut, Villigen, Switzerland
W. Bertl, K. Deiters, W. Erdmann, R. Horisberger, Q. Ingram, H.C. Kaestli, D. Kotlinski, U. Langenegger, T. Rohe, S.A. Wiederkehr

Institute for Particle Physics, ETH Zurich, Zurich, Switzerland
F. Bachmair, L. Bäni, L. Bianchini, B. Casal, G. Dissertori, M. Dittmar, M. Donegà, C. Grab, C. Heidegger, D. Hits, J. Hoss, G. Kasieczka, W. Lustermann, B. Mangano, M. Marionneau, P. Martinez Ruiz del Arbol, M. Masciovecchio, M.T. Meinhard, D. Meister, F. Micheli, P. Musella, F. Nessi-Tedaldi, F. Pandolfi, J. Pata, F. Pauss, G. Perrin, L. Perrozzi, M. Quittnat, M. Rossini, M. Schönenberger, A. Starodumov[47], V.R. Tavolaro, K. Theofilatos, R. Wallny

Universität Zürich, Zurich, Switzerland
T.K. Aarrestad, C. Amsler[48], L. Caminada, M.F. Canelli, A. De Cosa, S. Donato, C. Galloni, A. Hinzmann, T. Hreus, B. Kilminster, J. Ngadiuba, D. Pinna, G. Rauco, P. Robmann, D. Salerno, C. Seitz, Y. Yang, A. Zucchetta

National Central University, Chung-Li, Taiwan
V. Candelise, T.H. Doan, Sh. Jain, R. Khurana, M. Konyushikhin, C.M. Kuo, W. Lin, A. Pozdnyakov, S.S. Yu

National Taiwan University (NTU), Taipei, Taiwan
Arun Kumar, P. Chang, Y.H. Chang, Y. Chao, K.F. Chen, P.H. Chen, F. Fiori, W.-S. Hou, Y. Hsiung, Y.F. Liu, R.-S. Lu, M. Miñano Moya, E. Paganis, A. Psallidas, J.f. Tsai

Chulalongkorn University, Faculty of Science, Department of Physics, Bangkok, Thailand
B. Asavapibhop, K. Kovitanggoon, G. Singh, N. Srimanobhas

Cukurova University, Physics Department, Science and Art Faculty, Adana, Turkey
A. Adiguzel, F. Boran, S. Cerci[49], S. Damarseckin, Z.S. Demiroglu, C. Dozen, I. Dumanoglu, S. Girgis, G. Gokbulut, Y. Guler, I. Hos[50], E.E. Kangal[51], O. Kara, U. Kiminsu, M. Oglakci, G. Onengut[52], K. Ozdemir[53], D. Sunar Cerci[49], B. Tali[49], H. Topakli[54], S. Turkcapar, I.S. Zorbakir, C. Zorbilmez

Middle East Technical University, Physics Department, Ankara, Turkey
B. Bilin, G. Karapinar[55], K. Ocalan[56], M. Yalvac, M. Zeyrek

Bogazici University, Istanbul, Turkey
E. Gülmez, M. Kaya[57], O. Kaya[58], E.A. Yetkin[59]

Istanbul Technical University, Istanbul, Turkey
A. Cakir, K. Cankocak

Institute for Scintillation Materials of National Academy of Science of Ukraine, Kharkov, Ukraine
B. Grynyov

National Scientific Center, Kharkov Institute of Physics and Technology, Kharkov, Ukraine
L. Levchuk, P. Sorokin

University of Bristol, Bristol, United Kingdom
R. Aggleton, F. Ball, L. Beck, J.J. Brooke, D. Burns, E. Clement, D. Cussans, H. Flacher, J. Goldstein, M. Grimes, G.P. Heath, H.F. Heath, J. Jacob, L. Kreczko, C. Lucas, D.M. Newbold[60], S. Paramesvaran, A. Poll, T. Sakuma, S. Seif El Nasr-storey, D. Smith, V.J. Smith

Rutherford Appleton Laboratory, Didcot, United Kingdom
K.W. Bell, A. Belyaev[61], C. Brew, R.M. Brown, L. Calligaris, D. Cieri, D.J.A. Cockerill, J.A. Coughlan, K. Harder, S. Harper, E. Olaiya, D. Petyt, C.H. Shepherd-Themistocleous, A. Thea, I.R. Tomalin, T. Williams

Imperial College, London, United Kingdom
M. Baber, R. Bainbridge, O. Buchmuller, A. Bundock, S. Casasso, M. Citron, D. Colling, L. Corpe, P. Dauncey, G. Davies, A. De Wit, M. Della Negra, R. Di Maria, P. Dunne, A. Elwood, D. Futyan, Y. Haddad, G. Hall, G. Iles, T. James, R. Lane, C. Laner, L. Lyons, A.-M. Magnan, S. Malik, L. Mastrolorenzo, J. Nash, A. Nikitenko[47], J. Pela, M. Pesaresi, D.M. Raymond, A. Richards, A. Rose, E. Scott, C. Seez, S. Summers, A. Tapper, K. Uchida, M. Vazquez Acosta[62], T. Virdee[14], J. Wright, S.C. Zenz

Brunel University, Uxbridge, United Kingdom
J.E. Cole, P.R. Hobson, A. Khan, P. Kyberd, I.D. Reid, P. Symonds, L. Teodorescu, M. Turner

Baylor University, Waco, USA
A. Borzou, K. Call, J. Dittmann, K. Hatakeyama, H. Liu, N. Pastika

Catholic University of America, Washington, USA
R. Bartek, A. Dominguez

The University of Alabama, Tuscaloosa, USA
A. Buccilli, S.I. Cooper, C. Henderson, P. Rumerio, C. West

Boston University, Boston, USA
D. Arcaro, A. Avetisyan, T. Bose, D. Gastler, D. Rankin, C. Richardson, J. Rohlf, L. Sulak, D. Zou

Brown University, Providence, USA
G. Benelli, D. Cutts, A. Garabedian, J. Hakala, U. Heintz, J.M. Hogan, K.H.M. Kwok, E. Laird, G. Landsberg, Z. Mao, M. Narain, S. Piperov, S. Sagir, E. Spencer, R. Syarif

University of California, Davis, Davis, USA
D. Burns, M. Calderon De La Barca Sanchez, M. Chertok, J. Conway, R. Conway, P.T. Cox, R. Erbacher, C. Flores, G. Funk, M. Gardner, W. Ko, R. Lander, C. Mclean, M. Mulhearn, D. Pellett, J. Pilot, S. Shalhout, M. Shi, J. Smith, M. Squires, D. Stolp, K. Tos, M. Tripathi

University of California, Los Angeles, USA
M. Bachtis, C. Bravo, R. Cousins, A. Dasgupta, A. Florent, J. Hauser, M. Ignatenko, N. Mccoll, D. Saltzberg, C. Schnaible, V. Valuev

University of California, Riverside, Riverside, USA
E. Bouvier, K. Burt, R. Clare, J. Ellison, J.W. Gary, S.M.A. Ghiasi Shirazi, G. Hanson, J. Heilman, P. Jandir, E. Kennedy, F. Lacroix, O.R. Long, M. Olmedo Negrete, M.I. Paneva, A. Shrinivas, W. Si, H. Wei, S. Wimpenny, B. R. Yates

University of California, San Diego, La Jolla, USA
J.G. Branson, G.B. Cerati, S. Cittolin, M. Derdzinski, A. Holzner, D. Klein, G. Kole, V. Krutelyov, J. Letts, I. Macneill, D. Olivito, S. Padhi, M. Pieri, M. Sani, V. Sharma, S. Simon, M. Tadel, A. Vartak, S. Wasserbaech[63], F. Würthwein, A. Yagil, G. Zevi Della Porta

University of California, Santa Barbara - Department of Physics, Santa Barbara, USA
N. Amin, R. Bhandari, J. Bradmiller-Feld, C. Campagnari, A. Dishaw, V. Dutta, M. Franco Sevilla, C. George, F. Golf, L. Gouskos, J. Gran, R. Heller, J. Incandela, S.D. Mullin, A. Ovcharova, H. Qu, J. Richman, D. Stuart, I. Suarez, J. Yoo

California Institute of Technology, Pasadena, USA
D. Anderson, J. Bendavid, A. Bornheim, J.M. Lawhorn, H.B. Newman, C. Pena, M. Spiropulu, J.R. Vlimant, S. Xie, R.Y. Zhu

Carnegie Mellon University, Pittsburgh, USA
M.B. Andrews, T. Ferguson, M. Paulini, J. Russ, M. Sun, H. Vogel, I. Vorobiev, M. Weinberg

University of Colorado Boulder, Boulder, USA
J.P. Cumalat, W.T. Ford, F. Jensen, A. Johnson, M. Krohn, S. Leontsinis, T. Mulholland, K. Stenson, S.R. Wagner

Cornell University, Ithaca, USA
J. Alexander, J. Chaves, J. Chu, S. Dittmer, K. Mcdermott, N. Mirman, J.R. Patterson, A. Rinkevicius, A. Ryd, L. Skinnari, L. Soffi, S.M. Tan, Z. Tao, J. Thom, J. Tucker, P. Wittich, M. Zientek

Fairfield University, Fairfield, USA
D. Winn

Fermi National Accelerator Laboratory, Batavia, USA
S. Abdullin, M. Albrow, G. Apollinari, A. Apresyan, S. Banerjee, L.A.T. Bauerdick, A. Beretvas, J. Berryhill, P.C. Bhat, G. Bolla, K. Burkett, J.N. Butler, A. Canepa, H.W.K. Cheung, F. Chlebana, M. Cremonesi, J. Duarte, V.D. Elvira, I. Fisk, J. Freeman, Z. Gecse, E. Gottschalk, L. Gray, D. Green, S. Grünendahl, O. Gutsche, R.M. Harris, S. Hasegawa, J. Hirschauer, Z. Hu, B. Jayatilaka, S. Jindariani, M. Johnson, U. Joshi, B. Klima, B. Kreis, S. Lammel, D. Lincoln, R. Lipton, M. Liu, T. Liu, R. Lopes De Sá, J. Lykken, K. Maeshima, N. Magini, J.M. Marraffino, S. Maruyama, D. Mason, P. McBride, P. Merkel, S. Mrenna, S. Nahn, V. O'Dell, K. Pedro, O. Prokofyev, G. Rakness, L. Ristori, B. Schneider, E. Sexton-Kennedy, A. Soha, W.J. Spalding, L. Spiegel, S. Stoynev, J. Strait, N. Strobbe, L. Taylor, S. Tkaczyk, N.V. Tran, L. Uplegger, E.W. Vaandering, C. Vernieri, M. Verzocchi, R. Vidal, M. Wang, H.A. Weber, A. Whitbeck

University of Florida, Gainesville, USA
D. Acosta, P. Avery, P. Bortignon, A. Brinkerhoff, A. Carnes, M. Carver, D. Curry, S. Das, R.D. Field, I.K. Furic, J. Konigsberg, A. Korytov, K. Kotov, P. Ma, K. Matchev, H. Mei, G. Mitselmakher, D. Rank, L. Shchutska, D. Sperka, N. Terentyev, L. Thomas, J. Wang, S. Wang, J. Yelton

Florida International University, Miami, USA
S. Linn, P. Markowitz, G. Martinez, J.L. Rodriguez

Florida State University, Tallahassee, USA
A. Ackert, T. Adams, A. Askew, S. Hagopian, V. Hagopian, K.F. Johnson, T. Kolberg, T. Perry, H. Prosper, A. Santra, R. Yohay

Florida Institute of Technology, Melbourne, USA
M.M. Baarmand, V. Bhopatkar, S. Colafranceschi, M. Hohlmann, D. Noonan, T. Roy, F. Yumiceva

University of Illinois at Chicago (UIC), Chicago, USA
M.R. Adams, L. Apanasevich, D. Berry, R.R. Betts, R. Cavanaugh, X. Chen, O. Evdokimov, C.E. Gerber, D.A. Hangal, D.J. Hofman, K. Jung, J. Kamin, I.D. Sandoval Gonzalez, M.B. Tonjes, H. Trauger, N. Varelas, H. Wang, Z. Wu, J. Zhang

The University of Iowa, Iowa City, USA
B. Bilki[64], W. Clarida, K. Dilsiz[65], S. Durgut, R.P. Gandrajula, M. Haytmyradov, V. Khristenko, J.-P. Merlo, H. Mermerkaya[66], A. Mestvirishvili, A. Moeller, J. Nachtman, H. Ogul[67], Y. Onel, F. Ozok[68], A. Penzo, C. Snyder, E. Tiras, J. Wetzel, K. Yi

Johns Hopkins University, Baltimore, USA
B. Blumenfeld, A. Cocoros, N. Eminizer, D. Fehling, L. Feng, A.V. Gritsan, P. Maksimovic, J. Roskes, U. Sarica, M. Swartz, M. Xiao, C. You

The University of Kansas, Lawrence, USA
A. Al-bataineh, P. Baringer, A. Bean, S. Boren, J. Bowen, J. Castle, S. Khalil, A. Kropivnitskaya, D. Majumder, W. Mcbrayer, M. Murray, C. Royon, S. Sanders, R. Stringer, J.D. Tapia Takaki, Q. Wang

Kansas State University, Manhattan, USA
A. Ivanov, K. Kaadze, Y. Maravin, A. Mohammadi, L.K. Saini, N. Skhirtladze, S. Toda

Lawrence Livermore National Laboratory, Livermore, USA
F. Rebassoo, D. Wright

University of Maryland, College Park, USA
C. Anelli, A. Baden, O. Baron, A. Belloni, B. Calvert, S.C. Eno, C. Ferraioli, N.J. Hadley, S. Jabeen, G.Y. Jeng, R.G. Kellogg, J. Kunkle, A.C. Mignerey, F. Ricci-Tam, Y.H. Shin, A. Skuja, S.C. Tonwar

Massachusetts Institute of Technology, Cambridge, USA
D. Abercrombie, B. Allen, A. Apyan, V. Azzolini, R. Barbieri, A. Baty, R. Bi, K. Bierwagen, S. Brandt, W. Busza, I.A. Cali, M. D'Alfonso, Z. Demiragli, G. Gomez Ceballos, M. Goncharov, D. Hsu, Y. Iiyama, G.M. Innocenti, M. Klute, D. Kovalskyi, Y.S. Lai, Y.-J. Lee, A. Levin, P.D. Luckey, B. Maier, A.C. Marini, C. Mcginn, C. Mironov, S. Narayanan, X. Niu, C. Paus, C. Roland, G. Roland, J. Salfeld-Nebgen, G.S.F. Stephans, K. Tatar, D. Velicanu, J. Wang, T.W. Wang, B. Wyslouch

University of Minnesota, Minneapolis, USA
A.C. Benvenuti, R.M. Chatterjee, A. Evans, P. Hansen, S. Kalafut, S.C. Kao, Y. Kubota, Z. Lesko, J. Mans, S. Nourbakhsh, N. Ruckstuhl, R. Rusack, N. Tambe, J. Turkewitz

University of Mississippi, Oxford, USA
J.G. Acosta, S. Oliveros

University of Nebraska-Lincoln, Lincoln, USA
E. Avdeeva, K. Bloom, D.R. Claes, C. Fangmeier, R. Gonzalez Suarez, R. Kamalieddin, I. Kravchenko, J. Monroy, J.E. Siado, G.R. Snow, B. Stieger

State University of New York at Buffalo, Buffalo, USA
M. Alyari, J. Dolen, A. Godshalk, C. Harrington, I. Iashvili, A. Kharchilava, A. Parker, S. Rappoccio, B. Roozbahani

Northeastern University, Boston, USA
G. Alverson, E. Barberis, A. Hortiangtham, A. Massironi, D.M. Morse, D. Nash, T. Orimoto, R. Teixeira De Lima, D. Trocino, R.-J. Wang, D. Wood

Northwestern University, Evanston, USA
S. Bhattacharya, O. Charaf, K.A. Hahn, N. Mucia, N. Odell, B. Pollack, M.H. Schmitt, K. Sung, M. Trovato, M. Velasco

University of Notre Dame, Notre Dame, USA
N. Dev, M. Hildreth, K. Hurtado Anampa, C. Jessop, D.J. Karmgard, N. Kellams, K. Lannon, N. Loukas, N. Marinelli, F. Meng, C. Mueller, Y. Musienko[34], M. Planer, A. Reinsvold, R. Ruchti, N. Rupprecht, G. Smith, S. Taroni, M. Wayne, M. Wolf, A. Woodard

The Ohio State University, Columbus, USA
J. Alimena, L. Antonelli, B. Bylsma, L.S. Durkin, S. Flowers, B. Francis, A. Hart, C. Hill, W. Ji, B. Liu, W. Luo, D. Puigh, B.L. Winer, H.W. Wulsin

Princeton University, Princeton, USA
A. Benaglia, S. Cooperstein, O. Driga, P. Elmer, J. Hardenbrook, P. Hebda, D. Lange, J. Luo, D. Marlow, K. Mei, I. Ojalvo, J. Olsen, C. Palmer, P. Piroué, D. Stickland, A. Svyatkovskiy, C. Tully

University of Puerto Rico, Mayaguez, USA
S. Malik, S. Norberg

Purdue University, West Lafayette, USA
A. Barker, V.E. Barnes, S. Folgueras, L. Gutay, M.K. Jha, M. Jones, A.W. Jung, A. Khatiwada, D.H. Miller, N. Neumeister, J.F. Schulte, J. Sun, F. Wang, W. Xie

Purdue University Northwest, Hammond, USA
T. Cheng, N. Parashar, J. Stupak

Rice University, Houston, USA
A. Adair, B. Akgun, Z. Chen, K.M. Ecklund, F.J.M. Geurts, M. Guilbaud, W. Li, B. Michlin, M. Northup, B.P. Padley, J. Roberts, J. Rorie, Z. Tu, J. Zabel

University of Rochester, Rochester, USA
B. Betchart, A. Bodek, P. de Barbaro, R. Demina, Y.t. Duh, T. Ferbel, M. Galanti, A. Garcia-Bellido, J. Han, O. Hindrichs, A. Khukhunaishvili, K.H. Lo, P. Tan, M. Verzetti

The Rockefeller University, New York, USA
R. Ciesielski, K. Goulianos, C. Mesropian

Rutgers, The State University of New Jersey, Piscataway, USA
A. Agapitos, J.P. Chou, Y. Gershtein, T.A. Gómez Espinosa, E. Halkiadakis, M. Heindl, E. Hughes, S. Kaplan, R. Kunnawalkam Elayavalli, S. Kyriacou, A. Lath, R. Montalvo, K. Nash, M. Osherson, H. Saka, S. Salur, S. Schnetzer, D. Sheffield, S. Somalwar, R. Stone, S. Thomas, P. Thomassen, M. Walker

University of Tennessee, Knoxville, USA
M. Foerster, J. Heideman, G. Riley, K. Rose, S. Spanier, K. Thapa

Texas A&M University, College Station, USA
O. Bouhali[69], A. Castaneda Hernandez[69], A. Celik, M. Dalchenko, M. De Mattia, A. Delgado, S. Dildick, R. Eusebi, J. Gilmore, T. Huang, T. Kamon[70], R. Mueller, Y. Pakhotin, R. Patel, A. Perloff, L. Perniè, D. Rathjens, A. Safonov, A. Tatarinov, K.A. Ulmer

Texas Tech University, Lubbock, USA
N. Akchurin, J. Damgov, F. De Guio, C. Dragoiu, P.R. Dudero, J. Faulkner, E. Gurpinar, S. Kunori, K. Lamichhane, S.W. Lee, T. Libeiro, T. Peltola, S. Undleeb, I. Volobouev, Z. Wang

Vanderbilt University, Nashville, USA
S. Greene, A. Gurrola, R. Janjam, W. Johns, C. Maguire, A. Melo, H. Ni, P. Sheldon, S. Tuo, J. Velkovska, Q. Xu

University of Virginia, Charlottesville, USA
M.W. Arenton, P. Barria, B. Cox, R. Hirosky, A. Ledovskoy, H. Li, C. Neu, T. Sinthuprasith, X. Sun, Y. Wang, E. Wolfe, F. Xia

Wayne State University, Detroit, USA
C. Clarke, R. Harr, P.E. Karchin, J. Sturdy, S. Zaleski

University of Wisconsin - Madison, Madison, WI, USA
D.A. Belknap, J. Buchanan, C. Caillol, S. Dasu, L. Dodd, S. Duric, B. Gomber, M. Grothe, M. Herndon, A. Hervé, U. Hussain, P. Klabbers, A. Lanaro, A. Levine, K. Long, R. Loveless, G.A. Pierro, G. Polese, T. Ruggles, A. Savin, N. Smith, W.H. Smith, D. Taylor, N. Woods

1: Also at Vienna University of Technology, Vienna, Austria
2: Also at State Key Laboratory of Nuclear Physics and Technology, Peking University, Beijing, China
3: Also at Universidade Estadual de Campinas, Campinas, Brazil

4: Also at Universidade Federal de Pelotas, Pelotas, Brazil
5: Also at Université Libre de Bruxelles, Bruxelles, Belgium
6: Also at Joint Institute for Nuclear Research, Dubna, Russia
7: Also at Helwan University, Cairo, Egypt
8: Now at Zewail City of Science and Technology, Zewail, Egypt
9: Now at Fayoum University, El-Fayoum, Egypt
10: Also at British University in Egypt, Cairo, Egypt
11: Now at Ain Shams University, Cairo, Egypt
12: Also at Université de Haute Alsace, Mulhouse, France
13: Also at Skobeltsyn Institute of Nuclear Physics, Lomonosov Moscow State University, Moscow, Russia
14: Also at CERN, European Organization for Nuclear Research, Geneva, Switzerland
15: Also at RWTH Aachen University, III. Physikalisches Institut A, Aachen, Germany
16: Also at University of Hamburg, Hamburg, Germany
17: Also at Brandenburg University of Technology, Cottbus, Germany
18: Also at Institute of Nuclear Research ATOMKI, Debrecen, Hungary
19: Also at MTA-ELTE Lendület CMS Particle and Nuclear Physics Group, Eötvös Loránd University, Budapest, Hungary
20: Also at Institute of Physics, University of Debrecen, Debrecen, Hungary
21: Also at Indian Institute of Technology Bhubaneswar, Bhubaneswar, India
22: Also at Institute of Physics, Bhubaneswar, India
23: Also at University of Visva-Bharati, Santiniketan, India
24: Also at University of Ruhuna, Matara, Sri Lanka
25: Also at Isfahan University of Technology, Isfahan, Iran
26: Also at Yazd University, Yazd, Iran
27: Also at Plasma Physics Research Center, Science and Research Branch, Islamic Azad University, Tehran, Iran
28: Also at Università degli Studi di Siena, Siena, Italy
29: Also at Purdue University, West Lafayette, USA
30: Also at International Islamic University of Malaysia, Kuala Lumpur, Malaysia
31: Also at Malaysian Nuclear Agency, MOSTI, Kajang, Malaysia
32: Also at Consejo Nacional de Ciencia y Tecnología, Mexico city, Mexico
33: Also at Warsaw University of Technology, Institute of Electronic Systems, Warsaw, Poland
34: Also at Institute for Nuclear Research, Moscow, Russia
35: Now at National Research Nuclear University 'Moscow Engineering Physics Institute' (MEPhI), Moscow, Russia
36: Also at St. Petersburg State Polytechnical University, St. Petersburg, Russia
37: Also at University of Florida, Gainesville, USA
38: Also at P.N. Lebedev Physical Institute, Moscow, Russia
39: Also at California Institute of Technology, Pasadena, USA
40: Also at Budker Institute of Nuclear Physics, Novosibirsk, Russia
41: Also at Faculty of Physics, University of Belgrade, Belgrade, Serbia
42: Also at INFN Sezione di Roma; Sapienza Università di Roma, Rome, Italy
43: Also at University of Belgrade, Faculty of Physics and Vinca Institute of Nuclear Sciences, Belgrade, Serbia
44: Also at Scuola Normale e Sezione dell'INFN, Pisa, Italy
45: Also at National and Kapodistrian University of Athens, Athens, Greece
46: Also at Riga Technical University, Riga, Latvia
47: Also at Institute for Theoretical and Experimental Physics, Moscow, Russia

48: Also at Albert Einstein Center for Fundamental Physics, Bern, Switzerland
49: Also at Adiyaman University, Adiyaman, Turkey
50: Also at Istanbul Aydin University, Istanbul, Turkey
51: Also at Mersin University, Mersin, Turkey
52: Also at Cag University, Mersin, Turkey
53: Also at Piri Reis University, Istanbul, Turkey
54: Also at Gaziosmanpasa University, Tokat, Turkey
55: Also at Izmir Institute of Technology, Izmir, Turkey
56: Also at Necmettin Erbakan University, Konya, Turkey
57: Also at Marmara University, Istanbul, Turkey
58: Also at Kafkas University, Kars, Turkey
59: Also at Istanbul Bilgi University, Istanbul, Turkey
60: Also at Rutherford Appleton Laboratory, Didcot, United Kingdom
61: Also at School of Physics and Astronomy, University of Southampton, Southampton, United Kingdom
62: Also at Instituto de Astrofísica de Canarias, La Laguna, Spain
63: Also at Utah Valley University, Orem, USA
64: Also at BEYKENT UNIVERSITY, Istanbul, Turkey
65: Also at Bingol University, Bingol, Turkey
66: Also at Erzincan University, Erzincan, Turkey
67: Also at Sinop University, Sinop, Turkey
68: Also at Mimar Sinan University, Istanbul, Istanbul, Turkey
69: Also at Texas A&M University at Qatar, Doha, Qatar
70: Also at Kyungpook National University, Daegu, Korea